J. Fluid Mech. (1990), *vol.* 210, *pp.* 113–153
Printed in Great Britain

A stochastic model for the motion of particle pairs in isotropic high-Reynolds-number turbulence, and its application to the problem of concentration variance

By D. J. THOMSON†
Meteorological Office, London Road, Bracknell, Berkshire, RG12 2SZ

(Received 6 August 1987 and in revised form 16 June 1989)

A new stochastic model for the motion of particle pairs in isotropic high-Reynolds-number turbulence is proposed. The model is three-dimensional and its formulation takes account of recent improvements in the understanding of one-particle models. In particular the model is designed so that if the particle pairs are initially well mixed in the fluid, they will remain so. In contrast to previous models, the new model leads to a prediction for the particle separation probability density function which is in qualitative agreement with inertial subrange theory. The values of concentration variance from the model show encouraging agreement with experimental data. The model results suggest that, at large times, the intensity of concentration fluctuations (i.e. standard deviation of concentration divided by mean concentration) tends to zero in stationary conditions and to a constant in decaying turbulence.

1. Introduction

Although the behaviour of the ensemble average concentration of a passive tracer dispersing in a turbulent flow is quite well understood, there is still much to learn about concentration fluctuations. For example, there is no consensus in the literature on the value of the intensity of concentration fluctuations (i.e. standard deviation of concentration divided by mean concentration) at large times after a release, estimates of this quantity varying between zero and infinity (see, for example, the discussion given by Sawford & Hunt 1986). In spite of these problems, a number of techniques have been developed for the calculation of the concentration variance. None of these methods is exact, the complexity and nonlinearity of turbulent flows prohibiting the exact calculation of concentration statistics directly from the governing equations. Among the methods which deserve mention are high-order closure models (Newman, Launder & Lumley 1981; Sykes, Lewellen & Parker 1984), probability density function (p.d.f.) methods (Pope 1985; Anand & Pope 1985), stochastic models for the motions of particle-pairs (Durbin 1980) and two-point closure models (Lesieur 1987).

Concentration variance is intimately connected with the statistics of the trajectories of pairs of particles, and so stochastic models for the motion of particle pairs can be regarded as one of the more natural approaches to the problem. They have an advantage over the one-point high-order closure and p.d.f. methods in that the influence of the lengthscale of the concentration field is automatically accounted

† Also Department of Mathematics and Statistics, Brunel University.

for in a natural way. One consequence of this is that they can treat multiple sources, including the effect of correlations between the concentration from different sources. As indicated below, they can be regarded as a type of two-point closure model in which, in contrast to many more conventional two-point closures, no quasi-Gaussian assumption for the joint (two-point) p.d.f. of velocity and concentration is needed. Unlike p.d.f. methods, they do not seek to describe the probability distribution of the concentration, but merely its mean and variance.

The idea of using a model of the motion of particle pairs to estimate concentration variance via the numerical simulation of many particle-pair trajectories was first suggested in an imaginative and important paper by Durbin (1980). Since then such models have been discussed quite widely and have had some success in comparison with experimental data (Durbin 1982; Sawford 1985; Stapountzis *et al.* 1986). However, the correct way to formulate such models has not been investigated in detail. Recently a number of theoretical problems have been identified in connection with such models. For example, if the particle pairs in some of these models are well-mixed initially they will not remain so (Thomson 1986*b*). Also the majority of the models proposed to date are one-dimensional while the mixing processes which affect concentration variance are essentially three-dimensional. One consequence of this is that it is impossible to satisfy certain physical constraints in a one-dimensional model (Thomson 1986*b*). A number of two-particle models have been proposed to date (Durbin 1980; Lamb 1981; Sawford 1982; Gifford 1982; Lee & Stone 1983; Sawford & Hunt 1986), although the models of Gifford (1982) and Lee & Stone (1983) were intended for following clusters of particles rather than just pairs of particles. These models can be divided into two classes according to the predicted shape of the particle separation p.d.f. (Sawford 1983). The majority of the models (Lamb 1981; Sawford 1982; Gifford 1982; Lee & Stone 1983) predict that the p.d.f. is Gaussian (at least for initially coincident particles), while Durbin's (1980) model leads to a strongly peaked p.d.f. which tends to infinity at the origin. This difference in shape is important as it leads to very different predictions for the concentration fluctuations in some situations. Neither of these shapes seems very plausible, inertial subrange theory predicting that the p.d.f. should vary like $\alpha - \beta r^{\frac{2}{3}}$ near $r = 0$ (where r is the magnitude of the particle separation). This sheds some doubt on whether any of the stochastic models are showing the correct qualitative behaviour.

It is the thesis of this paper that some understanding of these problems can be obtained by considering recent developments in the theory of one-particle models (Van Dop, Nieuwstadt & Hunt 1985; Thomson 1987). These developments show that, in inhomogeneous turbulence, one-particle stochastic models can be badly in error unless they are formulated carefully. Consider, for example, a horizontally homogeneous situation with a vertical gradient in the vertical velocity variance σ_w^2. In such a situation the particles passing through a given point have a non-zero mean vertical acceleration even when there is no mean vertical Eulerian velocity. Failure to include this mean acceleration results in a situation where a tracer which is initially well mixed becomes 'un-mixed' and non-uniform in space at later times. The way in which such effects should be included in one-particle models is now well understood (Thomson 1987). Such problems are also likely to occur in two-particle models even in homogeneous turbulence. This is because of the variation of the two-point velocity covariance with the separation between the two points, something which is analogous to the variation of σ_w^2 with height in a one-particle model.

The aim of this paper is (i) to apply our understanding of one-particle models to the design of a three-dimensional two-particle model, (ii) to investigate whether such

a model overcomes the theoretical problems described above and results in a particle separation p.d.f. which is consistent with inertial subrange theory, and (iii) to compare the resulting predictions for concentration variance with experimental data. Some initial steps in this direction were taken by Thomson (1986*b*) using a one-dimensional model.

In §2 the basic ideas behind two-particle models and their relation to one-particle models are described, and in §3 the role of molecular diffusion in such models is discussed. The new two-particle model is described in §4 and its formulation is compared with that of other models. Some properties of the new model are investigated in §5, in particular the shape of the particle separation p.d.f. Finally, predictions for the concentration variance are presented and compared with experimental data in §6.

2. Basic concepts

It is useful to think of the tracer as consisting of many particles, a particle being an element of tracer which retains its identity. In the case of a particulate tracer, this agrees with the usual meaning of particle, while, in a tracer consisting of separate molecules, the particles are simply the molecules. The particles are assumed to be sufficiently small and numerous that the particle concentration can be regarded as a continuous quantity $c(\boldsymbol{x}, t)$. Only passive tracers will be considered here; more specifically, it is assumed that the presence of the tracer does not affect the velocity field $\boldsymbol{u}(\boldsymbol{x}, t)$ and that c satisfies the advection–diffusion equation

$$\partial c/\partial t + \boldsymbol{\nabla}\cdot(\boldsymbol{u}c) = \boldsymbol{\nabla}\cdot(\kappa\boldsymbol{\nabla}c), \tag{1}$$

where κ is the diffusivity resulting from random molecular (or Brownian) motions. In the following κ will be assumed constant. In Lagrangian terms, the assumptions embodied in (1) are equivalent to assuming that the particle trajectories $\boldsymbol{x}(t)$ satisfy the stochastic differential equation

$$\mathrm{d}\boldsymbol{x} = \boldsymbol{u}(\boldsymbol{x}, t)\,\mathrm{d}t + (2\kappa)^{\frac{1}{2}}\mathrm{d}\boldsymbol{\xi} \tag{2}$$

(Schuss 1980) where the components of $\mathrm{d}\boldsymbol{\xi}$ are the increments of independent Wiener processes (a Wiener process, sometimes called a Brownian motion, is a Gaussian process whose increments are independent with mean zero and variance $\mathrm{d}t$ – see e.g. Schuss 1980). In the following, molecular and Brownian motions are referred to as molecular for simplicity. Except where indicated the flow is assumed to be incompressible with constant density ρ.

The motion of pairs of particles plays a central role in the study of concentration fluctuations. Some insight into the motion of particle pairs can be achieved by regarding a particle pair whose particles are located at $\boldsymbol{x}_1$ and $\boldsymbol{x}_2$ as a single entity located at the point $\boldsymbol{X} = (\boldsymbol{x}_1, \boldsymbol{x}_2)$ in a six-dimensional space. It follows from (2) that the particle-pair trajectories $\boldsymbol{X}(t)$ are solutions of the stochastic differential equation

$$\mathrm{d}\boldsymbol{X} = \boldsymbol{U}(\boldsymbol{X}, t)\,\mathrm{d}t + (2\kappa)^{\frac{1}{2}}\mathrm{d}\boldsymbol{\xi}, \tag{3}$$

where $\boldsymbol{U}(\boldsymbol{X}, t)$ is the velocity field $(\boldsymbol{u}(\boldsymbol{x}_1, t), \boldsymbol{u}(\boldsymbol{x}_2, t))$ in $\boldsymbol{X}$-space. This result can also be expressed in Eulerian terms as follows. Let $C(\boldsymbol{X}, t)$ denote the concentration of particle pairs in $\boldsymbol{X}$-space. The number of particle pairs in the elemental volume $\mathrm{d}\boldsymbol{x}_1\,\mathrm{d}\boldsymbol{x}_2$ centred on $(\boldsymbol{x}_1, \boldsymbol{x}_2)$ in $\boldsymbol{X}$-space is equal to the product of the number of particles in the elemental volume $\mathrm{d}\boldsymbol{x}_1$ centred on $\boldsymbol{x}_1$ and the number in the volume $\mathrm{d}\boldsymbol{x}_2$ centred on $\boldsymbol{x}_2$. Hence $C(\boldsymbol{X}, t) = c(\boldsymbol{x}_1, t)\,c(\boldsymbol{x}_2, t)$. It follows from (1) that C satisfies

$$\partial C/\partial t + \boldsymbol{\nabla}\cdot(\boldsymbol{U}C) = \boldsymbol{\nabla}\cdot(\kappa\boldsymbol{\nabla}C). \tag{4}$$

This equation can also be derived directly as the Fokker–Planck equation of the process (3). Comparison of (1) and (4) or (2) and (3) shows that the particle pairs are advected and diffused in $\boldsymbol{X}$-space in the same way as single particles are advected and diffused in $\boldsymbol{x}$-space. In the following the first three and last three components of $\boldsymbol{U}$ will sometimes be denoted by $\boldsymbol{u}_1$ and $\boldsymbol{u}_2$ respectively, so that $\boldsymbol{U} = (\boldsymbol{u}_1, \boldsymbol{u}_2)$.

Throughout this paper we follow the statistical approach to turbulent flows, i.e. we regard the flow as a member of an ensemble of flows with identical external conditions (Monin & Yaglom 1971, p. 209) and consider only ensemble average quantities. Such averages will be denoted by angled brackets. The basic mathematical objects which arise in the statistical theory of turbulent dispersion are the n-particle transition probability distributions. Here we are only concerned with the first two of these which are defined as follows: $P_1(A, t\,|\,\boldsymbol{y}, s)$ is the probability of a particle trajectory, $\boldsymbol{x}(t)$, satisfying $\boldsymbol{x}(t) \in A$ given that $\boldsymbol{x}(s) = \boldsymbol{y}$, and $P_2(A_1, A_2, t_1, t_2\,|\,\boldsymbol{y}_1, \boldsymbol{y}_2, s_1, s_2)$ is the probability that two particle trajectories, $\boldsymbol{x}_i(t)$, $i = 1, 2$, satisfy $\boldsymbol{x}_i(t_i) \in A_i$ given that $\boldsymbol{x}_i(s_i) = \boldsymbol{y}_i$. A, A_1 and A_2 are subsets of Ω, the space occupied by the fluid. The p.d.f.s associated with the probability distributions P_1 and P_2 will be denoted by p_1 and p_2.

The reason why P_1 and P_2 are important quantities is that they determine the first- and second-order moments of c (see, for example, Egbert & Baker 1984). Consider a particular realization drawn from the ensemble of flows. In this realization, let $S(\boldsymbol{x}, t)$ be the source strength (i.e. the amount of tracer released per unit space–time volume). Although in many problems the source strength is deterministic (i.e. S is the same in every realization) it is useful to allow for the possibility of random sources (see Durbin 1982). In order to make progress, however, it is necessary to assume that S is independent of the flow field $\boldsymbol{u}$. In this case $\langle c(\boldsymbol{x}, t)\rangle$ and $\langle c(\boldsymbol{x}_1, t_1)\, c(\boldsymbol{x}_2, t_2)\rangle$ are given by

$$\langle c(\boldsymbol{x}, t)\rangle = \int_{s<t} p_1(\boldsymbol{x}, t\,|\,\boldsymbol{y}, s)\, S_1(\boldsymbol{y}, s)\, \mathrm{d}\boldsymbol{y}\, \mathrm{d}s \tag{5}$$

and

$$\langle c(\boldsymbol{x}_1, t_1)\, c(\boldsymbol{x}_2, t_2)\rangle = \int_{s_1<t_1,\, s_2<t_2} p_2(\boldsymbol{x}_1, \boldsymbol{x}_2, t_1, t_2\,|\,\boldsymbol{y}_1, \boldsymbol{y}_2, s_1, s_2)\, S_2(\boldsymbol{y}_1, \boldsymbol{y}_2, s_1, s_2)\, \mathrm{d}\boldsymbol{y}_1\, \mathrm{d}s_1\, \mathrm{d}\boldsymbol{y}_2\, \mathrm{d}s_2 \tag{6}$$

where $S_1(\boldsymbol{y}, s) = \langle S(\boldsymbol{y}, s)\rangle$ is the ensemble average source strength for particles of tracer and $S_2(\boldsymbol{y}_1, \boldsymbol{y}_2, s_1, s_2) = \langle S(\boldsymbol{y}_1, s_1)\, S(\boldsymbol{y}_2, s_2)\rangle$ is the ensemble average source strength for particle pairs. Equations (5) and (6) also hold in flows where ρ is not constant, although the condition that S is independent of the flow field $\boldsymbol{u}$ must be replaced by the requirement that S/ρ is independent of $\boldsymbol{u}$ and ρ (Thomson 1987).

As well as being of interest in their own right, knowledge of $\langle c(\boldsymbol{x}, t)\rangle$ and $\langle c(\boldsymbol{x}_1, t_1)\, c(\boldsymbol{x}_2, t_2)\rangle$ enables other quantities to be calculated. In many applications the average of $c(\boldsymbol{x}, t)$ over some space–time volume is of interest and the mean and variance of this quantity can be calculated. It is also possible to calculate the second-order moments of the spread of the cloud of tracer relative to its centre of mass from $\langle c(\boldsymbol{x}, t)\rangle$ and $\langle c(\boldsymbol{x}_1, t_1)\, c(\boldsymbol{x}_2, t_2)\rangle$ (Batchelor 1952).

p_1 and p_2 possess certain symmetry relations (Egbert & Baker 1984). Although this paper is only concerned with constant density flows it is useful to derive these relations in greater generality. This is because it enables us to obtain some insight into the model of Durbin (1980) which, although intended to represent diffusion in constant density flows, does not admit a well-mixed distribution of particle pairs

which is consistent with the constancy of ρ. Suppose that the tracer is well mixed in the fluid and choose a particle of tracer at random. Now consider the probability of it lying, at time t, in the elemental region $\mathrm{d}\boldsymbol{x}$ surrounding the point $\boldsymbol{x}$ and, at time s, in the region $\mathrm{d}\boldsymbol{y}$ surrounding the point $\boldsymbol{y}$. This probability is equal to the probability of it occupying the region $\mathrm{d}\boldsymbol{x}$ at time t given that it occupies $\mathrm{d}\boldsymbol{y}$ at time s (i.e. $p_1(\boldsymbol{x},t\,|\,\boldsymbol{y},s)\,\mathrm{d}\boldsymbol{x}$) times the probability of it occupying $\mathrm{d}\boldsymbol{y}$ at time s (i.e. $\langle\rho(\boldsymbol{y},s)\rangle\,\mathrm{d}\boldsymbol{y}/M$ where M is the total mass of the fluid). Hence the probability equals $p_1(\boldsymbol{x},t\,|\,\boldsymbol{y},s)\,\langle\rho(\boldsymbol{y},s)\rangle\,\mathrm{d}\boldsymbol{x}\,\mathrm{d}\boldsymbol{y}/M$. By symmetry, the probability is also given by $p_1(\boldsymbol{y},s\,|\,\boldsymbol{x},t)\,\langle\rho(\boldsymbol{x},t)\rangle\,\mathrm{d}\boldsymbol{x}\,\mathrm{d}\boldsymbol{y}/M$ and so

$$p_1(\boldsymbol{x},t\,|\,\boldsymbol{y},s)\,\langle\rho(\boldsymbol{y},s)\rangle = p_1(\boldsymbol{y},s\,|\,\boldsymbol{x},t)\,\langle\rho(\boldsymbol{x},t)\rangle. \tag{7}$$

Similarly, by considering a pair of particles chosen at random,

$$p_2(\boldsymbol{x}_1,\boldsymbol{x}_2,t_1,t_2\,|\,\boldsymbol{y}_1,\boldsymbol{y}_2,s_1,s_2)\,\langle\rho(\boldsymbol{y}_1,s_1)\,\rho(\boldsymbol{y}_2,s_2)\rangle$$
$$= p_2(\boldsymbol{y}_1,\boldsymbol{y}_2,s_1,s_2\,|\,\boldsymbol{x}_1,\boldsymbol{x}_2,t_1,t_2)\,\langle\rho(\boldsymbol{x}_1,t_1)\,\rho(\boldsymbol{x}_2,t_2)\rangle. \tag{8}$$

If ρ is constant, it follows that (5) and (6) can be expressed in the form

$$\langle c(\boldsymbol{x},t)\rangle = \int_{s<t} p_1(\boldsymbol{y},s\,|\,\boldsymbol{x},t)\,S_1(\boldsymbol{y},s)\,\mathrm{d}\boldsymbol{y}\,\mathrm{d}s$$

and

$$\langle c(\boldsymbol{x}_1,t_1)\,c(\boldsymbol{x}_2,t_2)\rangle = \int_{s_1<t_1,\,s_2<t_2} p_2(\boldsymbol{y}_1,\boldsymbol{y}_2,s_1,s_2\,|\,\boldsymbol{x}_1,\boldsymbol{x}_2,t_1,t_2)\,S_2(\boldsymbol{y}_1,\boldsymbol{y}_2,s_1,s_2)\,\mathrm{d}\boldsymbol{y}_1\,\mathrm{d}s_1\,\mathrm{d}\boldsymbol{y}_2\,\mathrm{d}s_2. \tag{9}$$

These equations are the so-called 'reverse' formulation of the 'forward' equations (5) and (6). In flows where ρ is not constant these equations are not valid and (9) must be replaced by

$$\frac{\langle c(\boldsymbol{x}_1,t_1)\,c(\boldsymbol{x}_2,t_2)\rangle}{\langle\rho(\boldsymbol{x}_1,t_1)\,\rho(\boldsymbol{x}_2,t_2)\rangle}$$
$$= \int_{s_1<t_1,\,s_2<t_2} p_2(\boldsymbol{y}_1,\boldsymbol{y}_2,s_1,s_2\,|\,\boldsymbol{x}_1,\boldsymbol{x}_2,t_1,t_2)\,\frac{S_2(\boldsymbol{y}_1,\boldsymbol{y}_2,s_1,s_2)}{\langle\rho(\boldsymbol{y}_1,s_1)\,\rho(\boldsymbol{y}_2,s_2)\rangle}\,\mathrm{d}\boldsymbol{y}_1\,\mathrm{d}s_1\,\mathrm{d}\boldsymbol{y}_2\,\mathrm{d}s_2. \tag{10}$$

In addition to these symmetry properties, P_1 and P_2 must obviously satisfy

$$P_1(A,t\,|\,\boldsymbol{y},s) = P_2(A,\Omega,t,t_2\,|\,\boldsymbol{y},\boldsymbol{y}_2,s,s_2). \tag{11}$$

The problem with (5) and (6) is that P_1 and P_2 cannot (with the present state of mathematical knowledge) be expressed exactly in terms of the Eulerian properties of the flow. Hence models are needed. One of the most natural approaches is to use stochastic models for the motion of single particles and particle pairs. Although single-particle models are now well understood and have been widely applied (e.g. Ley & Thomson 1983; Van Dop *et al.* 1985; De Baas *et al.* 1986; Thomson 1987), experience with two-particle models is much more limited. Because the particle pairs are advected and diffused in $\boldsymbol{X}$-space in the same way as single particles are in $\boldsymbol{x}$-space, it might be thought that the construction of a stochastic model for the motion of particle pairs would not be significantly more difficult than for single particles. However, there are some complications owing to the special nature of the flow field $\boldsymbol{U}$. Firstly, because the joint distribution of $\boldsymbol{u}(\boldsymbol{x}_1)$ and $\boldsymbol{u}(\boldsymbol{x}_2)$ depends on the separation $\boldsymbol{x}_1-\boldsymbol{x}_2$, the field $\boldsymbol{U}$ is always inhomogeneous, even in homogeneous turbulence. This is not a serious problem, but implies that the ideas developed for one-particle models

in inhomogeneous turbulence (Van Dop *et al.* 1985; Thomson 1987) need to be taken into account when designing a two-particle model. Secondly, the first three components of $\boldsymbol{U}$ are independent of $\boldsymbol{x}_2$ and the second three are independent of $\boldsymbol{x}_1$. This is a property of $\boldsymbol{U}$ which has no analogue in $\boldsymbol{u}$. Although this property results in some theoretical complications (see the end of §4.1), these appear to be unimportant in practice. Finally, if Γ denotes the subspace of points $\boldsymbol{X} = (\boldsymbol{x}_1, \boldsymbol{x}_2)$ with $\boldsymbol{x}_1 = \boldsymbol{x}_2$, then, at points in Γ, the direction of $\boldsymbol{U}$ lies within Γ (i.e. $\boldsymbol{u}(\boldsymbol{x}_1, t) = \boldsymbol{u}(\boldsymbol{x}_2, t)$ if $\boldsymbol{x}_1 = \boldsymbol{x}_2$), thereby preventing particle pairs escaping from the subspace Γ except by molecular diffusion. In other words, if the two particles in the pair are coincident†, they can only be separated by molecular processes. This complication is discussed in the next section.

3. Molecular diffusion in stochastic models

The formulation of stochastic models for the motion of single particles or particle pairs is complicated by the presence of molecular diffusion. In flows with high Reynolds (Re) and Péclet (Pe) numbers, such as the atmosphere, it seems very likely that, except very close to a small source, the effect of molecular diffusion on P_1 and $\langle c \rangle$ is small. Although this has not been proved rigorously, the intuitive argument given by Saffman (1960) is very convincing. Hence the one-particle models used to calculate P_1 and $\langle c \rangle$ can be formulated on the assumption that the particles of tracer move at the local velocity of the fluid.

The situation for two-particle models is rather more complex. Consider the motion of a particle pair with trajectory $\boldsymbol{X}(t) = (\boldsymbol{x}_1(t), \boldsymbol{x}_2(t))$ in $\boldsymbol{X}$-space. Re and Pe are assumed large. If the particle separation is large it seems likely, as in the one-particle case, that the effect of molecular diffusion on the motion of the particle pair is negligible in comparison to the effect of the turbulence. At large separations the fluid viscosity ν also has a negligible effect on the pair's motion because ν affects only the small-scale components of the turbulence. When the particles are close together however, $\boldsymbol{u}(\boldsymbol{x}_1, t) \approx \boldsymbol{u}(\boldsymbol{x}_2, t)$ and so molecular diffusion can have a significant effect on the particle separation; indeed if the two particles are coincident they can only separate by molecular processes. Also ν influences the small-scale components of the turbulence strongly and so will affect the motion of the particle pair when the separation is sufficiently small.

How small must the separation be for the effect of κ or ν to be significant? Let d be the maximum particle separation for which κ or ν has a significant effect on the motion of the pair of particles. Since we are assuming Re and Pe to be large, d will be much smaller than the outer length-scales of the turbulence. Hence, from Kolmogorov's theory of the universal equilibrium of the small-scale components of high-Reynolds-number turbulence (Monin & Yaglom 1975, chapter 8), d can depend only on κ, ν, and the ensemble average dissipation rate ϵ. Dimensional analysis then yields $d = f_1(Sc)\,(\nu^3/\epsilon)^{\frac{1}{4}}$ where f_1 is a function of the Schmidt number $Sc = \nu/\kappa$. If the particle separation is less than d, then the typical time taken for the particle separation to reach d will also depend only on κ, ν and ϵ, and will be of order $t_d = f_2(Sc)\,(\nu/\epsilon)^{\frac{1}{2}}$ where f_2 is another function of Sc. Once the particles have separated to a distance d any further separation is caused only by the turbulence occurring in

† 'Coincident' here and below means, of course, that the particle separation is small compared to all macroscopic scales and that both particles come from the same fluid element. It does not mean that the two particles are actually the same particle!

the inertial subrange and on larger scales; molecular diffusion no longer plays a significant role in the separation process.

For sufficiently large Re and fixed Sc, d and t_d can be made arbitrarily small compared with the outer lengthscales and timescales of the turbulence. It seems reasonable to expect that the precise manner in which the particle separation changes from zero to d (or vice versa) will not be important in calculating $\langle c(\boldsymbol{x}_1, t)\, c(\boldsymbol{x}_2, t)\rangle$; provided particles in the model are provided with the means to change their separation from zero to d in a time which is not greatly in excess of t_d, satisfactory results should be achieved. Following Durbin (1980), this can be achieved by ensuring that coincident particles can separate and by assuming that the inertial subrange of the turbulence in the model extends to arbitrarily large wavenumbers, so that if the separation of two particles is positive (no matter how small) they can be separated by the inertial subrange turbulence. The time required for inertial subrange turbulence to separate two particles to a distance d is, on dimensional grounds, of order $(d^2/\epsilon)^{\frac{1}{3}}$ which is, for fixed Sc, of order t_d. In a sense this procedure can be regarded as modelling not the real flow, but the flow which would occur in the limit $Re \to \infty$ with Sc and the outer lengthscales and timescales fixed. We will call this the high-Reynolds-number limit. The above procedure can also be justified by using the theory of the small-scale structure of scalar fields. The theory predicts that, for fixed values of Sc and the outer lengthscales and timescales and for sufficiently high Re, the value of $\langle c(\boldsymbol{x}_1, t)\, c(\boldsymbol{x}_2, t)\rangle$ is insensitive to the Reynolds number (Batchelor 1959; Batchelor, Howells & Townsend 1959; Monin & Yaglom 1975, chapter 8; Durbin, personal communication). It follows that the form of $\langle c(\boldsymbol{x}_1, t)\, c(\boldsymbol{x}_2, t)\rangle$ will converge to a limit as $Re \to \infty$ and, if the true Reynolds number is sufficiently high, the infinite-Reynolds-number form will be a good approximation to reality.

It should be pointed out that these arguments break down when considering measurements of $\langle c(\boldsymbol{x}_1, t)\, c(\boldsymbol{x}_2, t)\rangle$ at points close to small sources (i.e. points where the travel time from a source whose size is of order d or less is of order t_d or less). The precise value of κ is clearly important in such cases.

The above argument can hardly be called rigorous, but is very suggestive. Some support for the conclusion has been obtained from the two-particle model of Sawford & Hunt (1986) which includes diffusive and viscous effects explicitly. This model also gives an indication of how large Re must be (for a given Sc) for the high-Reynolds-number limit to be a good approximation. (Sawford & Hunt's model is based on that of Durbin (1980) which, as will be seen below, is not completely satisfactory. It would be of interest to repeat their work with a model based on that described in §4.1 below.)

4. A two-particle model, applicable in the high-Reynolds-number limit

In this section recent advances in the theory of one-particle models (Van Dop *et al.* 1985; Thomson 1987) are used to derive a model for the motion of particle pairs. For simplicity we consider only isotropic constant-density flows and always refer to a reference frame moving with the mean velocity. The Reynolds number is assumed to be large. This means, as indicated in the discussion in §3 above, that molecular diffusion can be neglected except when the two particles are coincident, and the inertial subrange of the turbulence can be assumed to extend to arbitrarily large wavenumbers. Except when the particles are coincident, the particles can be assumed to move at the local fluid velocity, i.e. as if they are fluid elements.

Let $\boldsymbol{X}(t) = (\boldsymbol{x}_1(t), \boldsymbol{x}_2(t))$ and $\boldsymbol{U}(t) = (\boldsymbol{u}_1(t), \boldsymbol{u}_2(t))$ be the position and velocity of the particle pair in $\boldsymbol{X}$-space. For convenience the same symbol $\boldsymbol{U}$ is used for the particle-pair velocity $\boldsymbol{U}(t)$ and the flow field $\boldsymbol{U}(\boldsymbol{X}, t)$; it should be clear from the context which is meant. Sometimes it is convenient, following Durbin (1980), to use an alternative coordinate system in which the components of $\boldsymbol{X}$ are related to the components of the separation vector $\boldsymbol{x}_1 - \boldsymbol{x}_2$ and the centroid $\boldsymbol{x}_1 + \boldsymbol{x}_2$. If we define $\Delta\boldsymbol{x} = (\boldsymbol{x}_1 - \boldsymbol{x}_2)/\sqrt{2}$, $\Sigma\boldsymbol{x} = (\boldsymbol{x}_1 + \boldsymbol{x}_2)/\sqrt{2}$, $\Delta\boldsymbol{u} = (\boldsymbol{u}_1 - \boldsymbol{u}_2)/\sqrt{2}$ and $\Sigma\boldsymbol{u} = (\boldsymbol{u}_1 + \boldsymbol{u}_2)/\sqrt{2}$, then, in the new rotated coordinate system, $\boldsymbol{X} = (\Delta\boldsymbol{x}, \Sigma\boldsymbol{x})$ and $\boldsymbol{U} = (\Delta\boldsymbol{u}, \Sigma\boldsymbol{u})$. In the sequel, $\Delta\boldsymbol{x}$ will often, for simplicity, be referred to as 'the particle separation', ignoring the factor $1/\sqrt{2}$. Superscripts will denote Cartesian components and the summation convection will be used. The superscripts will run from 1 to 3 or from 1 to 6 depending on whether they refer to a three-dimensional quantity (such as $\boldsymbol{x}_1$ or $\Delta\boldsymbol{u}$) or a six-dimensional one (such as $\boldsymbol{X}$). $g(\boldsymbol{X}, \boldsymbol{U}, t)$ will denote the density function of the distribution of contaminant particle pairs in $(\boldsymbol{X}, \boldsymbol{U})$-space at time t and $g_a(\boldsymbol{X}, \boldsymbol{U}, t)$ will denote the corresponding density function for all pairs of fluid elements. Since the fluid has constant density, $\int g_a \, d\boldsymbol{U}$ is independent of $\boldsymbol{X}$ and $g_a(\boldsymbol{X}, \boldsymbol{U}, t)$ is proportional to the p.d.f. of the velocity $\boldsymbol{U}(\boldsymbol{X}, t)$, i.e. g_a contains the same information as the two-point velocity statistics.

$(\boldsymbol{X}, \boldsymbol{U})$ is assumed to be a Markov process, i.e. given the values of $\boldsymbol{X}$ and $\boldsymbol{U}$ at time t, the values at times greater than t are independent of the values at times less than t. Although this may not be exactly true it is a reasonable assumption to make. This is because, in high-Reynolds-number turbulence, the acceleration of a fluid element has a significant autocorrrelation only over very short time intervals of the order of the Kolmogorov timescale $\tau_\eta = (\nu/\epsilon)^{\frac{1}{2}}$ (Monin & Yaglom 1975, §21.5) and, in the high-Re limit (discussed in §3), $\tau_\eta \to 0$. Hence the changes in $\boldsymbol{U}(t)$ over successive time intervals Δt are only weakly correlated. Of course they cannot be completely independent or the variance of $\boldsymbol{U}$ would grow indefinitely. In making the Markovian assumption it is assumed that this dependence can be accounted for by allowing the velocity increments to depend on the particle pair's velocity and position. Given some regularity assumptions on the Markov process it follows that $(\boldsymbol{X}, \boldsymbol{U})$ satisfies a pair of stochastic differential equations of the form

$$\mathrm{d}\boldsymbol{X} = \boldsymbol{U}\,\mathrm{d}t, \tag{12a}$$

$$\mathrm{d}U^i = a^i(\boldsymbol{X}, \boldsymbol{U}, t)\,\mathrm{d}t + b^{ij}(\boldsymbol{X}, \boldsymbol{U}, t)\,\mathrm{d}\xi^j, \tag{12b}$$

where, as in (2), the components of $\mathrm{d}\boldsymbol{\xi}$ are the increments of independent Wiener processes (see e.g. Schuss 1980). B^{ij} will be used to denote $\frac{1}{2}b^{ik}b^{jk}$. Although $\boldsymbol{B}$ does not determine $\boldsymbol{b}$, it does determine the distribution of the random increments $b^{ij}\,\mathrm{d}\xi^j$; hence the specification of $\boldsymbol{a}$ and $\boldsymbol{B}$ is sufficient to determine the way the particle pairs move. It follows from (12) that g evolves according to the Fokker–Planck equation,

$$\frac{\partial g}{\partial t} = -\frac{\partial}{\partial X^i}(U^i g) - \frac{\partial}{\partial U^i}(a^i g) + \frac{\partial^2}{\partial U^i \partial U^j}(B^{ij} g). \tag{13}$$

4.1. *The choice of* $\boldsymbol{a}$ *and* $\boldsymbol{B}$

As indicated above, $\boldsymbol{a}$ and $\boldsymbol{B}$ will be selected by applying the theoretical ideas developed previously for one-particle models (Van Dop *et al.* 1985; Thomson 1987).

In order to apply these ideas we need to assume a form for the density function g_a. For simplicity g_a is assumed to be Gaussian with

$$\left.\begin{aligned}\langle u_1^i u_1^j\rangle &= \langle u_2^i u_2^j\rangle = \sigma^2\delta^{ij},\\ \langle u_1^i u_2^j\rangle &= \langle u_2^i u_1^j\rangle = \sigma^2 R^{ij}(\Delta\boldsymbol{x}),\end{aligned}\right\} \tag{14}$$

or, equivalently,

$$\left.\begin{aligned}\langle \Delta u^i \Delta u^j\rangle &= \sigma^2(\delta^{ij} - R^{ij}(\Delta\boldsymbol{x})),\\ \langle \Sigma u^i \Sigma u^j\rangle &= \sigma^2(\delta^{ij} + R^{ij}(\Delta\boldsymbol{x})),\\ \langle \Delta u^i \Sigma u^j\rangle &= 0\end{aligned}\right\} \tag{15}$$

(here $\boldsymbol{u}_1$, $\Delta\boldsymbol{u}$ etc. indicate the components of the field $\boldsymbol{U}(\boldsymbol{X}, t)$, not the velocity $\boldsymbol{U}(t)$ of a particle pair). $\boldsymbol{R}$ is the two-point velocity correlation tensor. Because of incompressibility, $\partial R^{ij}/\partial\Delta x^j = 0$ (Batchelor 1953, p. 27) and, since $\boldsymbol{R}$ is isotropic, it can be written in the form

$$R^{ij} = F(\Delta)\,\Delta x^i\,\Delta x^j + G(\Delta)\,\delta^{ij},$$

where $\Delta = |\Delta\boldsymbol{x}|$ and F and G satisfy $4F + \Delta\,\partial F/\partial\Delta + (1/\Delta)\,\partial G/\partial\Delta = 0$. Following Durbin (1980) we take the longitudinal correlation function, $f = F\Delta^2 + G$, to be

$$f = 1 - (\Delta^2/(\Delta^2 + l^2))^{\frac{1}{3}}. \tag{16}$$

This form is qualitatively reasonable and gives the correct inertial subrange form at small Δ. The integral scale L of f, $\int f(\Delta)\,\mathrm{d}(\Delta\sqrt{2})$, is equal to $1.06\,l$. In the inertial subrange $f = 1 - C(\epsilon\Delta\sqrt{2})^{\frac{2}{3}}/(2\sigma^2)$ (Monin & Yaglom 1975, p. 353) where C is the Kolmogorov constant which is taken here to be 2.0 (Monin & Yaglom 1975, p. 485). Hence, in terms of σ^2 and ϵ, $l = \sigma^3/(\epsilon\sqrt{2})$. This is consistent with the longitudinal integral scale being of order $0.8\sigma^3/\epsilon$ (Townsend 1976, p. 61). F and G can be calculated from f. The six-dimensional covariance tensor $\langle U^i U^j\rangle$ will be denoted by V^{ij}. The various components of $\boldsymbol{V}$ are given, in the $(\boldsymbol{x}_1, \boldsymbol{x}_2)$ coordinate system, by (14) and, in the rotated $(\Delta\boldsymbol{x}, \Sigma\boldsymbol{x})$ coordinate system, by (15). In reality g_a is not Gaussian, especially when Δ is small (Batchelor 1953, pp. 170–173), and it is hard to assess the error incurred by assuming that it is. This deserves further investigation. Of course the model does not assume that the velocity and concentration fields are jointly Gaussian and allows the mixed velocity–concentration two-point third-order moments to be non-zero. This is essential in any model of $\langle c^2\rangle$ since

$$\langle c(\boldsymbol{x}_1)\,c(\boldsymbol{x}_2)\,\boldsymbol{U}(\boldsymbol{X})\rangle = \langle C(\boldsymbol{X})\,\boldsymbol{U}(\boldsymbol{X})\rangle$$

represents the flux of pairs of contaminant particles in $\boldsymbol{X}$-space.

In reality, if the tracer is well mixed in the fluid at some time, then it will also be well mixed at all subsequent times. Hence, in a realistic model, if g is proportional to g_a at some time, it should remain so (the 'well-mixed condition'). This implies that g_a should satisfy (13) and this in turn leads to constraints on $\boldsymbol{a}$ and $\boldsymbol{B}$. The theory presented by Thomson (1987) for one-particle models extends easily to two-particle models and shows that a two-particle model will be consistent with many aspects of the dispersion physics provided that it satisfies the well-mixed condition. In particular, this condition ensures that the small-time behaviour of g for dispersion from an instantaneous source is correct, that the relation (8) between the forward

and reverse formulations is satisfied whenever $t_1 = t_2$ and $s_1 = s_2$, and that the model is equivalent to a two-point closure assumption on terms of the form

$$\langle c(\boldsymbol{x}_1)\, c(\boldsymbol{x}_2)\, u^i(\boldsymbol{x}_1) \dots u^m(\boldsymbol{x}_1)\, u^n(\boldsymbol{x}_2) \dots u^q(\boldsymbol{x}_2)\, (\mathrm{D}\boldsymbol{u}(\boldsymbol{x}_1)/\mathrm{D}t)\rangle,$$

where $\mathrm{D}\boldsymbol{u}/\mathrm{D}t = \partial\boldsymbol{u}/\partial t + \boldsymbol{u}\cdot\boldsymbol{\nabla}\boldsymbol{u}$. Because the assumed form of g_a is consistent (and indeed only consistent) with an ensemble of flows in which the fluid density is constant, the well-mixed condition also ensures that the model is consistent with a number of consequences of the constant density constraint. For example it satisfies $p_2(\boldsymbol{x}_1, \boldsymbol{x}_2, t, t \,|\, \boldsymbol{y}_1, \boldsymbol{y}_2, s, s) = p_2(\boldsymbol{y}_1, \boldsymbol{y}_2, s, s \,|\, \boldsymbol{x}_1, \boldsymbol{x}_2, t, t)$, a consequence of (8) for constant density flows. This does not, of course, imply that the model is necessarily completely consistent with the constant density constraint in the strong sense discussed by Thomson (1987, §3.6).

In order to satisfy the well-mixed condition it is necessary and sufficient for $\boldsymbol{a}$ to satisfy

$$a^i g_a = \partial(B^{ij} g_a)/\partial U^j + \phi^i, \tag{17a}$$

for some $\boldsymbol{\phi}$ satisfying

$$\partial\phi^i/\partial U^i = -\partial g_a/\partial t - \partial(U^i g_a)/\partial X^i \tag{17b}$$

and

$$\boldsymbol{\phi} \to 0 \quad \text{as } |\boldsymbol{U}| \to \infty \tag{17c}$$

(Thomson 1987). For our value of g_a,

$$\frac{\phi^i}{g_a} = \frac{1}{2}\frac{\partial V^{il}}{\partial X^l} + \tfrac{1}{2}(\boldsymbol{V}^{-1})^{ij}\frac{\partial V^{il}}{\partial t}U^j + \tfrac{1}{2}(\boldsymbol{V}^{-1})^{ij}\frac{\partial V^{il}}{\partial X^k}U^j U^k \tag{18}$$

is perhaps the simplest choice of $\boldsymbol{\phi}$ satisfying (17b) and (17c) (Thomson 1987). In our situation the term $\frac{1}{2}\partial V^{il}/\partial X^l$ is in fact zero because of the constant density constraint on $\boldsymbol{R}$.

$\boldsymbol{B}$ remains to be chosen. In one-particle models the choice of $\boldsymbol{B}$ is well understood (Obukhov 1959; Novikov 1963; Monin & Yaglom 1975, p. 547, pp. 571–573; Van Dop *et al.* 1985; Haworth & Pope 1986; Pope 1987; Thomson 1987). In choosing $\boldsymbol{B}$ for our two-particle model we will be guided by the one-particle case and also by ideas about the motion of particle pairs discussed by Novikov (1963) and Monin & Yaglom (1975, p. 573). In high Re flows the acceleration correlation function is short-ranged in space as well as time (Monin & Yaglom 1975, §21.5) and so the acceleration of any particle is only weakly correlated with that of any other. However the accelerations cannot be completely independent or, at large times, all the particles would be moving independently. In (12), the acceleration of the first particle in a pair of particles consists of two parts, a^i and $b^{ij}\,\mathrm{d}\xi^j/\mathrm{d}t$, $i = 1, 2, 3$. It seems reasonable to suppose that the part of the acceleration which is uncorrelated from one moment to the next, namely $b^{ij}\,\mathrm{d}\xi^j/\mathrm{d}t$, is also uncorrelated with the position, velocity or acceleration of the other particle. Also, for simplicity and consistency with inertial subrange theory, we would like $\boldsymbol{B}$ to be independent of $\boldsymbol{U}$ (see Thomson (1987, §4) for a discussion of the analogous one-particle case). Together with the assumed isotropy of the turbulence, this leads to the choice $B^{ij} = B\delta^{ij}$. Because B represents the high-frequency part of the acceleration, it should depend only on ϵ, i.e. $B = \frac{1}{2}C_0\epsilon$ for some C_0. For short time intervals $[s, t]$, (12) then implies that the one-particle Lagrangian structure function

$$D^{ij} = \overline{(u_1^i(t) - u_1^i(s))\,(u_1^j(t) - u_1^j(s))}$$

takes the form $C_0\epsilon\delta^{ij}(t-s)$, the overbar indicating an average over all particles with a given position at time s (or, equivalently, over all particle pairs with a given $\boldsymbol{x}_1(s)$).

Hence C_0 can be identified with the universal constant occurring in the inertial subrange part of $\boldsymbol{D}$. There is great uncertainty in the value of C_0 but the data of Hanna (1981) support a value of 4.0 ± 2.0 (C_0 is Hanna's $2\pi^2 B$). In this paper C_0 will be taken to be 4.0. In the following B will often be written as σ^2/τ. It will be shown below that τ can be interpreted as a Lagrangian timescale. Because $\boldsymbol{B}$ remains constant as $\Delta \to 0$ the model allows particles to separate and no special measures are needed to ensure this. With the above value of $\boldsymbol{B}$ and with $\boldsymbol{\phi}$ given by (18), (17a) becomes

$$a^i = -\frac{\sigma^2}{\tau}(\boldsymbol{V}^{-1})^{ij} U^j + \tfrac{1}{2}(\boldsymbol{V}^{-1})^{lj}\frac{\partial V^{il}}{\partial t} U^j + \tfrac{1}{2}(\boldsymbol{V}^{-1})^{lj}\frac{\partial V^{il}}{\partial X^k} U^j U^k.$$

To complete the specification of the model, we note that the initial value of $\boldsymbol{U}$ for a particle pair commencing at $(\boldsymbol{y}_1, \boldsymbol{y}_2)$ at time s is chosen at random from the two-point velocity distribution at $(\boldsymbol{y}_1, \boldsymbol{y}_2)$.

When the particles are far apart, the particles move independently and the motion of a single particle obeys the stochastic differential equations

$$\left.\begin{aligned} \mathrm{d}\boldsymbol{x}_1 &= \boldsymbol{u}_1 \,\mathrm{d}t, \\ \mathrm{d}\boldsymbol{u}_1 &= \left(-\frac{1}{\tau} + \frac{1}{\sigma}\frac{\partial \sigma}{\partial t}\right)\boldsymbol{u}_1 \,\mathrm{d}t + \sigma\left(\frac{2}{\tau}\right)^{\frac{1}{2}} \mathrm{d}\xi. \end{aligned}\right\} \tag{19}$$

This is an appropriate model for the motion of a single particle in isotropic Gaussian turbulence and satisfies a one-particle version of the well-mixed condition (Thomson 1987). Equation (19) can be expressed more simply as

$$\left.\begin{aligned} \mathrm{d}\boldsymbol{x}_1 &= \sigma \tilde{\boldsymbol{u}}_1 \,\mathrm{d}t, \\ \mathrm{d}\tilde{\boldsymbol{u}}_1 &= -(\tilde{\boldsymbol{u}}_1/\tau)\,\mathrm{d}t + (2/\tau)^{\frac{1}{2}} \mathrm{d}\xi, \end{aligned}\right\} \tag{20}$$

where $\tilde{\boldsymbol{u}}_1 = \boldsymbol{u}_1/\sigma$. In stationary situations this is simply a three-dimensional version of the Langevin equation and so $\overline{u_1^i(t)\, u_1^j(s)} = \sigma^2 \delta^{ij} \exp\left(-(t-s)/\tau\right)$. Hence τ is the Lagrangian *integral* timescale of the model. $C_0 = 4.0$ implies $\tau\sigma/L = 0.67$ which is within the scatter of observed values (Pasquill & Smith 1983, §2.7). In non-stationary conditions τ is not the *integral* timescale, but is simply a measure of the timescale on which particle velocities become decorrelated.

The above model has been designed to be consistent with g_a and can claim to be more faithful in this respect than previous models. However, it is not completely satisfactory as it ignores one aspect of the field $\boldsymbol{U}(\boldsymbol{X}, t)$ which is not reflected in g_a, namely the fact that $\boldsymbol{u}_1$ does not depend on $\boldsymbol{x}_2$ and $\boldsymbol{u}_2$ does not depend on $\boldsymbol{x}_1$. Consider for the moment a single realization of the flow and consider the trajectory $\boldsymbol{X}(t) = (\boldsymbol{x}_1(t), \boldsymbol{x}_2(t))$ of the pair of fluid elements for which, at time s, the first element is at $\boldsymbol{y}_1$ and the second at $\boldsymbol{y}_2$. From this trajectory $\boldsymbol{X}(t) = (\boldsymbol{x}_1(t), \boldsymbol{x}_2(t))$ we can obtain a single particle trajectory $\boldsymbol{x}_1(t)$ in $\boldsymbol{x}$-space. This trajectory satisfies $\mathrm{d}\boldsymbol{x}_1/\mathrm{d}t = \boldsymbol{u}_1(\boldsymbol{X}, t)$ and $\boldsymbol{x}_1(s) = \boldsymbol{y}_1$. Because of the property of $\boldsymbol{U}$ described above, $\boldsymbol{u}_1$ depends only on $\boldsymbol{x}_1$ and t and hence the single particle trajectory obtained would be the same, no matter what value $\boldsymbol{y}_2$ takes. If we now consider the ensemble of such particle and particle-pair trajectories occurring in the ensemble of flows (one particle or particle-pair trajectory for each member of the ensemble) it is clear that,

For fixed $\boldsymbol{y}_1$, the ensemble of trajectories $\boldsymbol{x}_1(t)$ is the same for all choices of $\boldsymbol{y}_2$ (21)

(this is a strengthened version of (11)). The trajectories of the particle pairs from the above model do not satisfy this. For example, consider the evolution of $\overline{u_1^i(t)\, u_1^i(t)}$ and

$\overline{u_2^i(t)\,u_2^i(t)}$ for particle pairs with position $(\boldsymbol{y}_1, \boldsymbol{y}_2)$ in $\boldsymbol{X}$-space at time s. If $|\boldsymbol{y}_1 - \boldsymbol{y}_2| \gg l$, the particles move according to (19) and it follows that

$$\overline{u_1^i(t)\,u_1^i(t)} = \overline{u_2^i(t)\,u_2^i(t)} = 3\sigma^2. \tag{22}$$

If the model is to satisfy (21), then (22) must be true for all initial separations and hence $\overline{U^i(t)\,U^i(t)} = 6\sigma^2$ for all initial separations. However, using either the Fokker–Planck equation (13) or Itô's formula (see e.g. Schuss 1980), the above model yields

$$\overline{U^i(t)\,U^i(t)} = 6\sigma^2 - \sigma^4(F\Delta^2(2\Delta\,\mathrm{d}F/\mathrm{d}\Delta + 5F))_{\Delta=|\boldsymbol{y}_1-\boldsymbol{y}_2|/\sqrt{2}}(t-s)^2 + O((t-s)^3), \tag{23}$$

showing that the model trajectories do indeed violate (21) (it is easy to see that $F\Delta^2(2\Delta\,\mathrm{d}F/\mathrm{d}\Delta + 5F)$ cannot be identically zero).

It is of interest to ask if the model can be modified to satisfy (21) and the well-mixed condition by choosing a different form for $\boldsymbol{\phi}$ (the physical reasoning leading to the choice of $\boldsymbol{B}$ given above is strong and so we do not wish to alter the form of $\boldsymbol{B}$). Although it may be possible to choose $\boldsymbol{\phi}$ so that $\overline{U^i(t)\,U^i(t)}$ is correct to order $(t-s)^2$, the author thinks it is unlikely that $\boldsymbol{\phi}$ can be chosen so that $\overline{U^i(t)\,U^i(t)}$ is correct to all orders, and hence even less likely that $\boldsymbol{\phi}$ can be chosen so that (21) is satisfied. The author has however been unable to prove the impossibility of satisfying both (21) and the well-mixed condition.

Although the fact that the model violates (21) is a little unsatisfactory, the results of a number of numerical simulations, presented below, suggest that this is not too serious in practice.

In the calculations of mean and mean square concentration presented in §6 below, it is convenient to follow the particles backwards and to use (9) to calculate $\langle c^2 \rangle$ at a point (the point from which the trajectories start). When the trajectories are evaluated in the forward direction, only the mean square of c averaged over some finite sample volume can be obtained since a large number of pair trajectories need to pass through the receptor to reduce statistical error. For the isotropic Gaussian turbulence considered in this paper the calculation of the reverse trajectories is straightforward. Let $(\boldsymbol{X}'(t), \boldsymbol{U}'(t))$ denote the ensemble of forward trajectories starting at $(\boldsymbol{Y}, -\boldsymbol{V})$ at time $-s$ calculated from the model with $\sigma(t)$, $l(t)$, $\epsilon(t)$ and $\tau(t)$ replaced by $\sigma(-t)$, $l(-t)$, $\epsilon(-t)$ and $\tau(-t)$ respectively. The theory presented by Thomson (1987) implies that the ensemble of trajectories $(\boldsymbol{X}(t), \boldsymbol{U}(t)) = (\boldsymbol{X}'(-t), -\boldsymbol{U}'(-t))$ is the required ensemble of backwards trajectories starting at $(\boldsymbol{Y}, \boldsymbol{V})$ at time s.

4.2. *Comparison with other models*

It is appropriate to compare the above choice of $\boldsymbol{a}$ and $\boldsymbol{B}$ with the values adopted in other models. Perhaps the simplest two-particle model of the form (12) is the following. For a pair of particles originating at position $(\boldsymbol{y}_1, \boldsymbol{y}_2)$ in $\boldsymbol{X}$-space at time s, choose the initial velocities to be correlated, with $\overline{u_1^i u_2^j} = \sigma^2 R^{ij}((\boldsymbol{y}_1 - \boldsymbol{y}_2)/\sqrt{2})$. To be consistent with our assumptions about g_a, we choose $\boldsymbol{u}_1$ and $\boldsymbol{u}_2$ to be jointly Gaussian. Subsequently each particle moves independently according to (19). We will call this the NGLS model since it owes much to the ideas of Novikov (1963), Gifford (1982) and Lee & Stone (1983) (see also Lin & Reid 1963), although it is not identical to the models proposed by these authors. For example, Novikov (1963) only makes assumptions about the second moments of quantities while Gifford (1982) and Lee & Stone (1983) only consider the component of the motion in one direction, restrict consideration to stationary conditions and do not make any specific assumption

about the form of the initial velocity distribution. In addition the models of Gifford (1982) and Lee & Stone (1983) were intended to be used for following clusters of particles rather than just two particles, but can of course be applied to the problem of the dispersion of particle pairs. We will adopt the NGLS model as a representative example of the class of models which yield a Gaussian p.d.f. for the separation of a pair of particles which are initially coincident (i.e. the models of Lamb 1981; Sawford 1982; Gifford 1982; Lee & Stone 1983).

The NGLS model has the advantage of satisfying (21); indeed, together with a number of variants, it is the only model of the form (12) proposed to date which satisfies (21). However, it does not satisfy the well-mixed condition, at least not with any physically reasonable form for g_a; if the two particles approach closely at some time after release, the model will not ensure that they have similar velocities. Of course the NGLS equations for the evolution of the particle-pair trajectories are consistent with the form $g_a \propto \sigma^{-6}\exp(-U^iU^i/2\sigma^2)$, but this form is unrealistic in that it implies zero correlation between velocities at neighbouring points. Also the initial velocity distribution of the particle pairs is not consistent with this form.

A two-particle model which has been widely applied is the one-dimensional model of Durbin (1980). The extension of this model to non-stationary conditions (suggested by Durbin and reported in Stapountzis *et al.* (1986)) takes the form

$$\left.\begin{aligned} \mathrm{d}\Delta x &= \Delta\tilde{u}\,\sigma(1-f)^{\frac{1}{2}}\,\mathrm{d}t, \\ \mathrm{d}\Sigma x &= \Sigma\tilde{u}\,\sigma(1+f)^{\frac{1}{2}}\,\mathrm{d}t, \\ \mathrm{d}\Delta\tilde{u} &= -(\Delta\tilde{u}/\tau)\,\mathrm{d}t + (2/\tau)^{\frac{1}{2}}\,\mathrm{d}\xi, \\ \mathrm{d}\Sigma\tilde{u} &= -(\Sigma\tilde{u}/\tau)\,\mathrm{d}t + (2/\tau)^{\frac{1}{2}}\,\mathrm{d}\xi', \end{aligned}\right\} \tag{24}$$

where $\Delta\tilde{u} = \Delta u/(\sigma(1-f)^{\frac{1}{2}})$, $\Sigma\tilde{u} = \Sigma u/(\sigma(1+f)^{\frac{1}{2}})$, ξ and ξ' are independent Wiener processes and the correlation function f has the form (16). In the same way as (19) was expressed in the form (20), it is straightforward to express Durbin's model in the form (12) although the equations then appear more complex. The initial values of $\Delta\tilde{u}$ and $\Sigma\tilde{u}$ are chosen to be independent and Gaussian with variance 1. Because this model is one-dimensional, it is appropriate to comment on the physical interpretation of Δx and Σx. In most of the applications of the model that have been made to date (Durbin 1980; Sawford 1983, 1985; Sawford & Hunt 1986), the values of Δx and Σx are interpreted as the values of one component (say the x-component) of $\Delta\boldsymbol{x}$ and $\Sigma\boldsymbol{x}$, and attention is restricted to source distributions which are homogeneous in the y- and z-directions. Equation (24) is then used as a model for the backwards trajectories (with t in (24) interpreted as running in the opposite direction to real time) and the second moments of c are calculated from the statistics of such trajectories using a one-dimensional version of (9):

$$\langle c(x_1,t)\,c(x_2,t)\rangle = \int_{s_1<t,\,s_2<t} p_2(y_1,y_2,s_1,s_2\,|\,x_1,x_2,t,t)\,S_2(y_1,y_2,s_1,s_2)\,\mathrm{d}y_1\,\mathrm{d}s_1\,\mathrm{d}y_2\,\mathrm{d}s_2. \tag{25}$$

This equation can be derived from (9) if the trajectories defined by (24) are interpreted as trajectories for particle pairs whose initial separations in the y- and z-directions are zero and $\langle c(x_1,t)\,c(x_2,t)\rangle$ is interpreted as the covariance of the concentrations at two points which have the same y and z coordinates.

Like the NGLS model, Durbin's model does not satisfy the well-mixed condition

with a physically reasonable form of g_a. As in the NGLS model, there is a form of g_a which is consistent with Durbin's model, namely

$$g_a \propto \frac{1}{\sigma^2(1-f)(1+f)^{\frac{1}{2}}} \exp\left(-\frac{(\Delta u)^2}{2\sigma^2(1-f)} - \frac{(\Sigma u)^2}{2\sigma^2(1+f)}\right),$$

but this form implies infinite $\langle \rho^2 \rangle$. Related to this fact is the fact that, if $\langle c^2 \rangle$ is calculated using forward trajectories and a one-dimensional version of (6), then, for a contaminant that is initially uniform in space (in every realization), the model predicts that $\langle c^2 \rangle$ will be infinite at all times after release (Sawford 1983; Egbert & Baker 1984). This problem is avoided by using the backwards relation (25) which automatically ensures that fluctuations will not appear if the initial conditions are well-mixed. Of course (25) was derived from (9) which was in turn derived on the assumption that ρ is constant, and so, because the model's well-mixed state is not consistent with a constant ρ, there is an inconsistency between (24) and (25). Like the new model proposed above, Durbin's model fails to satisfy (21). To see this note that particle pairs released at (y_1, y_2) have an initial mean relative acceleration unless $|y_1 - y_2| \gg l$ (Thomson 1986*b*).

5. Properties of P_2

We can learn something about the new model described in §4.1 by looking at some of the properties of P_2 as predicted by the model. One of the most important quantities that can be calculated from P_2 is the distribution of the particle separation $\Delta \boldsymbol{x}$. $p_\Delta(\Delta \boldsymbol{x}, t \mid s)$ will be used to denote the p.d.f. of $\Delta \boldsymbol{x}$ at time t for particle pairs with zero separation at time s, i.e.

$$p_\Delta(\Delta \boldsymbol{x}, t \mid s) = \int p_2((\Sigma \boldsymbol{x} + \Delta \boldsymbol{x})/\sqrt{2}, (\Sigma \boldsymbol{x} - \Delta \boldsymbol{x})/\sqrt{2}, t, t \mid 0, 0, s, s)\, \mathrm{d}\Sigma \boldsymbol{x}.$$

Because we are considering isotropic turbulence, this p.d.f. is a function of $\Delta = |\Delta \boldsymbol{x}|$ only and so is sometimes written as $p_\Delta(\Delta, t \mid s)$ or, if it is clear what values t and s take, as $p_\Delta(\Delta)$. However this is not the p.d.f. of Δ which is equal to $4\pi\Delta^2 p_\Delta(\Delta)$. The reason why p_Δ is an important quantity is that it has a strong effect on the mean square concentration, with strongly peaked shapes leading to larger values of the mean square concentration (Sawford 1983). In the same way $p_\Sigma(\Sigma \boldsymbol{x}, t \mid s)$ will denote the p.d.f. of $\Sigma \boldsymbol{x}$ at time t for particle pairs with both particles coincident at the origin at time s. This is a function of $\Sigma = |\Sigma \boldsymbol{x}|$ only and so will sometimes be written as $p_\Sigma(\Sigma, t \mid s)$. In addition, for particle pairs with both particles at the origin at time s, the distributions of $\boldsymbol{x}_1$, $\Delta \boldsymbol{x}$ and $\Sigma \boldsymbol{x}$ are spherically symmetric. For this case $\sigma_1(t \mid s)$, $\sigma_\Delta(t \mid s)$ and $\sigma_\Sigma(t \mid s)$ will be used to denote the root-mean-square value of one component of $\boldsymbol{x}_1$, $\Delta \boldsymbol{x}$ and $\Sigma \boldsymbol{x}$ respectively at time t. For one-dimensional models such as Durbin's (1980), the above definitions do not apply directly. We note here that, in such models, p_Δ, p_Σ, σ_Δ and σ_Σ will be used to denote the p.d.f.s and mean-square values of Δx and Σx for particle pairs which are coincident at the origin at time s.

In the following we will investigate the properties of P_2 from the new model for both stationary and decaying turbulence. These properties will be compared with the properties of some of the other models described in §4.2.

5.1. *Stationary turbulence*

Let us first consider the idealized case where the turbulence is stationary. Only forward trajectory statistics will be described here; because the flow is stationary,

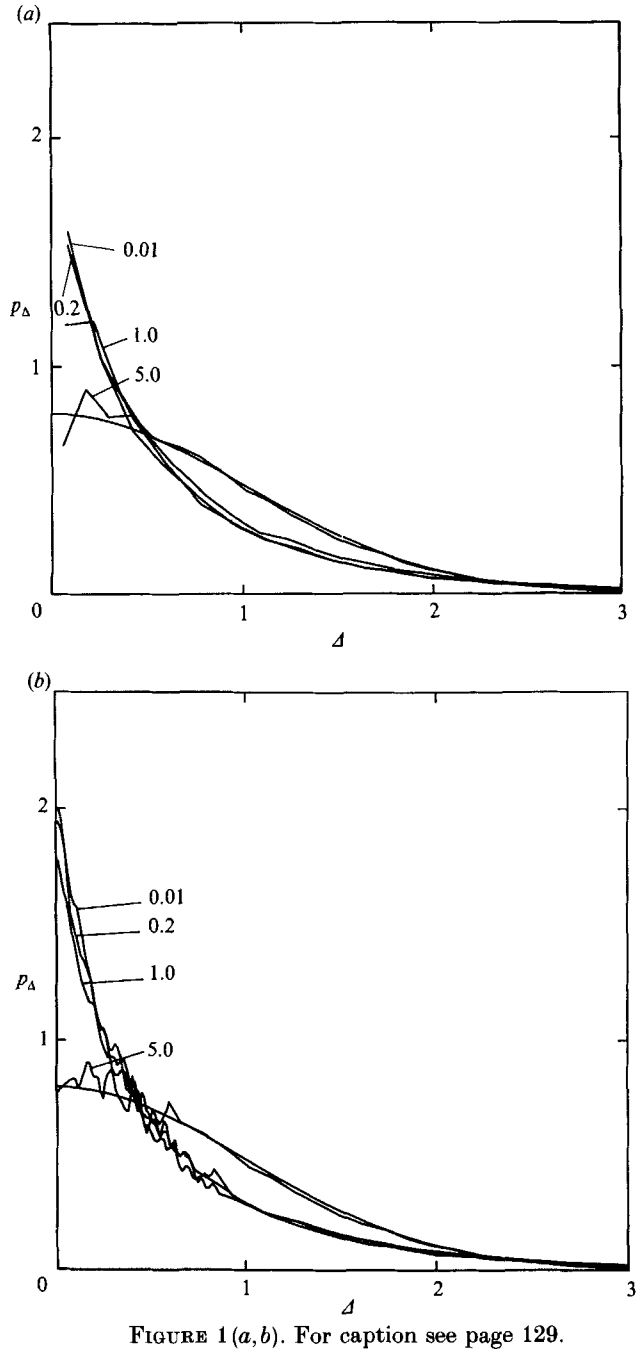

FIGURE 1 (*a*, *b*). For caption see page 129.

the discussion at the end of §4.1 implies that these statistics can also be interpreted as the statistics of backward trajectories. Figure 1 (*a*) shows the p.d.f. of the distribution of $\Delta \boldsymbol{x}$ in the new model at time t for zero separation at time s. Unfortunately, p_Δ cannot be calculated analytically and so numerical results are shown. The details of the numerical calculations are given in Appendix A. In fact, in the numerical simulations it is impossible to start with particles which are truly

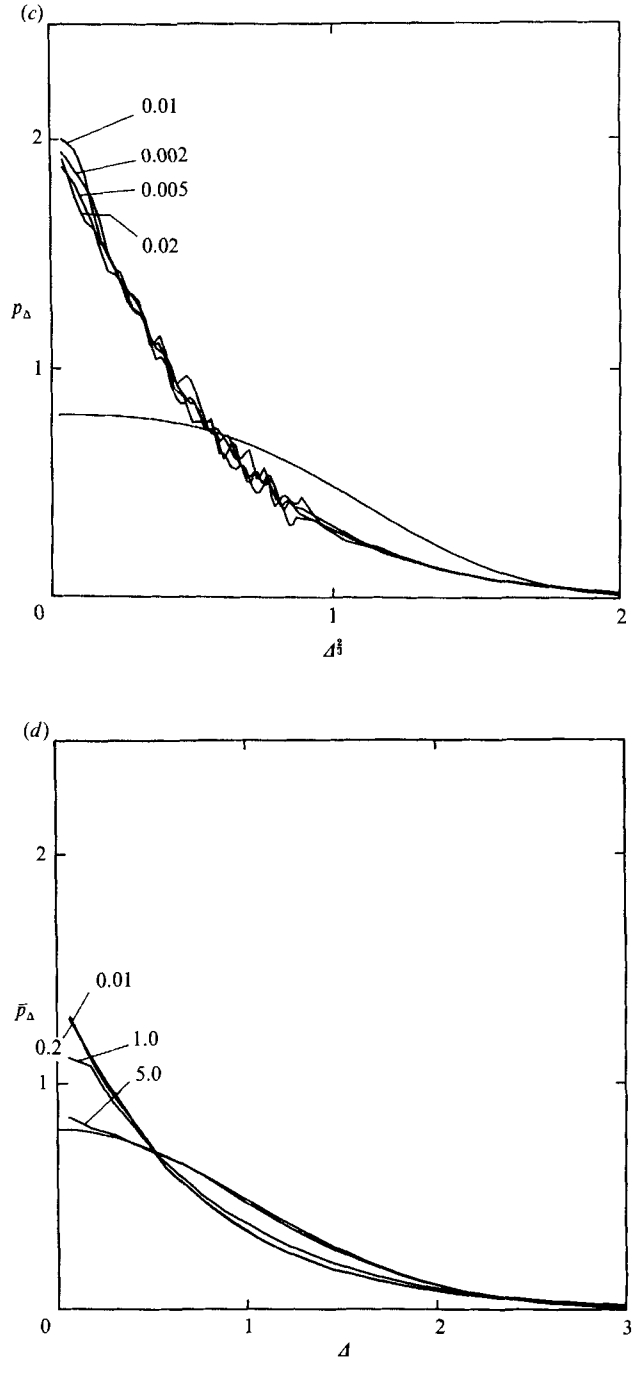

FIGURE 1 (*c*, *d*). For caption see facing page.

coincident, and so a small initial separation equal to $2 \times 10^{-6} l$ was used. The results are insensitive to changes in this quantity of an order of magnitude. This is discussed further in Appendix A. The curves shown consist of straight lines between a number of data points, each data point representing the average value of p_Δ over a small interval of Δ values. It can be seen that the distribution changes from a strongly

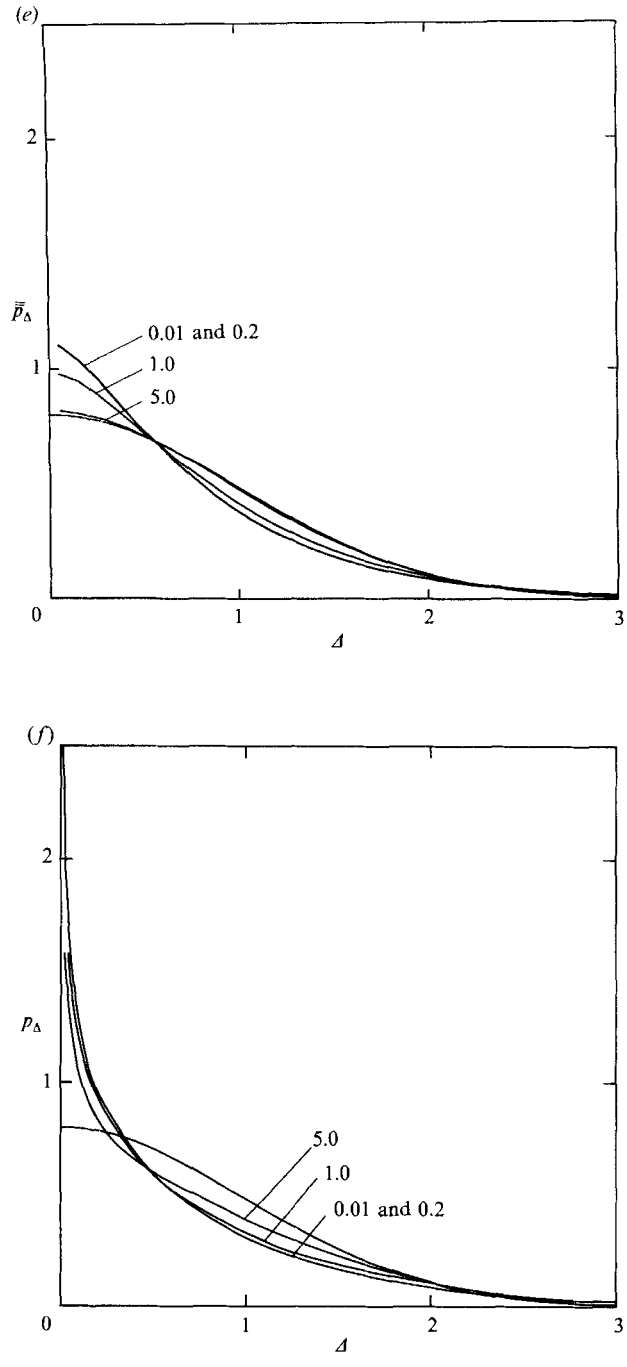

FIGURE 1. The shape of $p_\Delta(\Delta, t \mid s)$ in stationary turbulence. The curves are normalized with zeroth and second moments equal to unity as if they were one-dimensional p.d.f.s (*a*)–(*e*) show the results for the new model: (*a*) shows the results obtained without 'particle splitting', (*b*) shows results obtained using the particle-splitting technique, (*c*) shows results obtained using the particle-splitting technique plotted against $\Delta^{\frac{2}{3}}$ to show the $\alpha - \beta\Delta^{\frac{2}{3}}$ behaviour near $\Delta = 0$, (*d*) shows $\bar{p}_\Delta(\Delta, t \mid s)$ and (*e*) shows $\bar{p}_\Delta(\Delta, t \mid s)$. (*f*) shows p_Δ from Durbin's (1980) model. The numbers attached to the curves indicate values of $t-s$ normalized by σ^2/ϵ, and the unlabelled line is a Gaussian distribution.

peaked distribution to a Gaussian distribution as t increases. This was also observed by Thomson (1986*b*) using what is essentially a one-dimensional version of the model. At small times, $t-s \ll \tau$, the shape is independent of t. This is to be expected on dimensional grounds because, from inertial subrange theory, p_Δ should depend only on Δ, $t-s$ and ϵ.

One of the problems of having to calculate p_Δ numerically is that it is very difficult to obtain an accurate value for $p_\Delta(0)$. This is because very few particle pairs pass sufficiently close to $\Delta = 0$ and so the results show a great deal of statistical scatter. In order to obtain a better estimate of p_Δ near the origin, the following 'particle splitting' technique was applied. Each particle pair is assigned a weight which indicates the importance to be attached to the pair in calculating the statistics. Whenever, for any integer n in the range 0 to 18, the separation of the particles becomes less than $\Delta_n = \sigma_\Delta 2^{n/3} \times 10^{-2}$, having been greater than Δ_n in the previous timestep, the particle pair is divided into two copies which then move independently, each pair being given a weight equal to half the weight assigned to the parent particle pair. Similarly, whenever the separation of the particles becomes greater than Δ_n (having been less than Δ_n in the previous step) the pair has a probability of $\frac{1}{2}$ of being annihilated. If the particle pair survives, the weighting assigned to it is doubled. This method ensures that there are a lot of particle pairs with small separations, each having a very small weight. A proof showing that this does not introduce a bias into the results but merely alters the accuracy is given in Thomson (1988). The value of σ_Δ which was used in defining Δ_n was obtained from the calculations made without the particle-splitting technique. The result is shown in figure 1(*b*). Because of the increased accuracy at small separations, it is possible to place the data points from which the curves are constructed closer together. In order to resolve the behaviour near $\Delta = 0$, the data points have been placed as close together as is possible without the scatter becoming unacceptable. More accurate results could be obtained by following a greater number of particles; however, as with all Monte Carlo methods, the convergence is slow, the error decreasing as $N^{-\frac{1}{2}}$ where N is the number of particle pairs.

It is clear from (6) that $p_\Delta(\Delta\boldsymbol{x}, t\,|\,s)$ is equal to the value of $\langle c(\boldsymbol{x},t)\,c(\boldsymbol{x}+\Delta\boldsymbol{x}\sqrt{2},t)\rangle$ resulting from an initially isotropic concentration field with

$$\langle c(\boldsymbol{x},s)\,c(\boldsymbol{x}+\Delta\boldsymbol{x}\sqrt{2},s)\rangle = \delta(\Delta\boldsymbol{x})$$

where δ is the Dirac delta function. Now, for Δ lying in the inertial subrange, classical theory (e.g. Monin & Yaglom 1975, p. 384) predicts that the concentration covariance function $\langle c(\boldsymbol{x},t)\,c(\boldsymbol{x}+\Delta\boldsymbol{x}\sqrt{2},t)\rangle$ has the form $\alpha-\beta\Delta^{\frac{2}{3}}$. Hence p_Δ should also have this form for small Δ. The model results for small $t-s$ do indeed agree with this, as is shown by the straight-line behaviour near the origin in figure 1(*c*). At larger $t-s$ (not shown in figure 1*c*) the inertial subrange behaviour ceases to be apparent in the graph of p_Δ; this is to be expected because the region in which the inertial subrange form should occur ($\Delta \ll l$) becomes small relative to the lengthscale σ_Δ on which p_Δ varies.

Figures 1(*d*) and 1(*e*) show the p.d.f.s of $(\Delta x^2, \Delta x^3)$ and of Δx^3. These are functions of $((\Delta x^2)^2+(\Delta x^3)^2)^{\frac{1}{2}}$ and $|\Delta x^3|$ respectively, and will be written as $\bar{p}_\Delta(\Delta)$ and $\bar{\bar{p}}_\Delta(\Delta)$ where Δ is to be interpreted, with a slight abuse of notation, as $((\Delta x^2)^2+(\Delta x^3)^2)^{\frac{1}{2}}$ or $|\Delta x^3|$. They are closer to a Gaussian distribution than p_Δ, the peak in p_Δ at small separations being smoothed by the process of integrating p_Δ over Δx^1 or over Δx^1 and Δx^2. (The use of superscripts for Cartesian components becomes a bit clumsy here, but appears unavoidable – subscripts are already used for distinguishing between

particles 1 and 2 and the use of y and z for x^2 and x^3 is liable to be confused with the use of $\boldsymbol{x}$ and $\boldsymbol{y}$ to denote two points in space.)

In both Durbin's (1980) model and the NGLS model, p_Δ can be calculated analytically. In Durbin's model, p_Δ is always strongly peaked and infinite at $\Delta = 0$ as shown in figure 1(f). In the NGLS model p_Δ is exactly Gaussian at all times. The similarity in the shape of p_Δ at times $t-s \ll \tau$ in the new model and the model of Durbin is striking. However, the difference in behaviour near the origin has some important consequences. Firstly the new model can treat the problem of a point source and does not require the explicit treatment of molecular diffusion which is needed to smooth the singularity in Durbin's model (Sawford & Hunt 1986). Also, because of the shapes of p_Δ and p_Σ (see below for discussion of p_Σ) and the fact that σ_Δ and σ_Σ tend to infinity as $t-s \to \infty$, it follows that, for any given lengthscale, the values of p_Δ and p_Σ from the new model will show little variation on this scale when $t-s$ is sufficiently large. It seems reasonable to suppose the same is also true of the quantity $p_2(\boldsymbol{x}_1, \boldsymbol{x}_2, t, t \,|\, \boldsymbol{y}, \boldsymbol{y}, s, s)$, and hence (using the above-noted fact that the model statistics for forward and backward trajectories are equal in stationary conditions) of the quantity $p_2(\boldsymbol{y}_1, \boldsymbol{y}_2, s, s \,|\, \boldsymbol{x}, \boldsymbol{x}, t, t)$. Now, for an instantaneous spatially-bounded deterministic source, (9) can be written as

$$\langle c(\boldsymbol{x}, t)^2 \rangle = \int p_2(\boldsymbol{y}_1, \boldsymbol{y}_2, s, s \,|\, \boldsymbol{x}, \boldsymbol{x}, t, t) S(\boldsymbol{y}_1) S(\boldsymbol{y}_2) \, \mathrm{d}\boldsymbol{y}_1 \, \mathrm{d}\boldsymbol{y}_2,$$

where s is the time at which the contaminant is released (S here has a slightly different meaning to the S introduced in §2, being the amount of tracer released per unit volume, not per unit space–time volume). It follows from the above property of the quantity $p_2(\boldsymbol{y}_1, \boldsymbol{y}_2, s, s \,|\, \boldsymbol{x}, \boldsymbol{x}, t, t)$ that this can be approximated when $t-s$ is large by

$$\langle c(\boldsymbol{x}, t)^2 \rangle = p_2(\boldsymbol{y}, \boldsymbol{y}, s, s \,|\, \boldsymbol{x}, \boldsymbol{x}, t, t) \int S(\boldsymbol{y}_1) S(\boldsymbol{y}_2) \, \mathrm{d}\boldsymbol{y}_1 \, \mathrm{d}\boldsymbol{y}_2,$$

where $\boldsymbol{y}$ is some point in the source region. Hence, provided the total amount of material released remains fixed, $\langle c^2 \rangle$ becomes independent of source size in the new model. Similar arguments, using $\bar{p}_\Delta$ or $\bar{\bar{p}}_\Delta$ instead of p_Δ, show that $\langle c^2 \rangle$ becomes independent of source 'size' (i.e. source thickness) for instantaneous area and line sources also. In contrast, the value of $p_2(\boldsymbol{y}_1, \boldsymbol{y}_2, s, s \,|\, \boldsymbol{x}, \boldsymbol{x}, t, t)$ in Durbin's model shows variations on a lengthscale l or less at all times owing to the singularity in p_Δ. Hence, as discussed by Durbin (1980) and Sawford (1983), $\langle c^2 \rangle$ never becomes independent of the source size for sources of size less than l. Although it is not clear how to prove from first principles that this behaviour is wrong, it seems intuitively very unlikely.

A partial justification of the idea that $\langle c^2 \rangle$ should become independent of source size is possible by considering the equality noted above between $p_\Delta(\Delta\boldsymbol{x}, t \,|\, s)$ and the spatial covariance function of a hypothetical isotropic concentration field. We have already noted that this implies $p_\Delta \approx \alpha - \beta \Delta^{\frac{2}{3}}$ for Δ lying in the inertial subrange. Now at large times σ_Δ^2 grows like t and so α cannot decrease faster than $t^{-\frac{3}{2}}$. Now α is the variance of our hypothetical concentration field and β is proportional to its rate of dissipation (see e.g. Monin & Yaglom 1975, p. 384). Hence β/α must become small, since otherwise α would decrease exponentially. It follows that p_Δ is likely to show little variation on small scales for large $t-s$. In addition it seems likely that p_Σ will also show little variation on small scales at large $t-s$ (see discussion of p_Σ below). Hence, for the same reasons as given above in discussing the behaviour of $\langle c^2 \rangle$ in the model, it seems likely that the value of $\langle c^2 \rangle$ for instantaneous plane, line or compact sources will become independent of source size at large times.

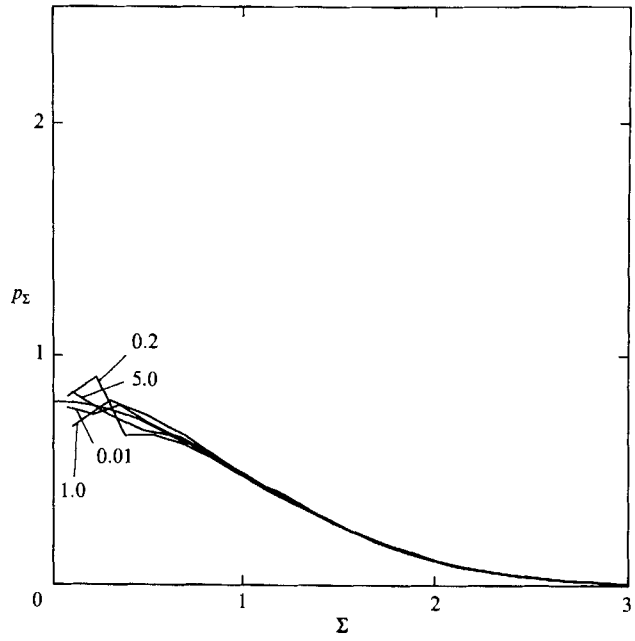

FIGURE 2. The shape of $p_\Sigma(\Sigma, t|s)$ from the new model in stationary turbulence. The curves are normalized with zeroth and second moments equal to unity as if they were one-dimensional p.d.f.s The numbers attached to the curves indicate values of $t-s$ normalized by σ^2/ϵ, and the unlabelled line is a Gaussian distribution.

It should be pointed out that, in most of the applications of Durbin's model made to date (Durbin 1980; Sawford 1983, 1985; Sawford & Hunt 1986), p_Δ is, as noted in §4.2, interpreted as the p.d.f. of one component of $\Delta \boldsymbol{x}$ (this is the logical interpretation since the model is one-dimensional). Hence it should be compared with the value of $\bar{\bar{p}}_\Delta$ from the new model (figure 1*e*). If this is done, the agreement in shape is much worse. It is not proposed here to investigate in detail how much of this difference is due to the one-dimensionality of Durbin's model and how much is a result of the failure to satisfy the 'well-mixed condition'. However, for $t-s \ll \tau$, the model of Thomson (1986*b*) (which is essentially a one-dimensional version of the model of §4.1 and which satisfies the well-mixed condition) also shows a much stronger peak at $\Delta = 0$ than does $\bar{\bar{p}}_\Delta$ from the new model, suggesting that the one-dimensionality of Durbin's model may be an important factor.

Figure 2 shows the p.d.f. of the distribution of $\Sigma \boldsymbol{x}$. In the new model it is close to Gaussian at all times. As in figure 1, the scatter at small Σ is statistical noise. The value of p_Σ in the NGLS model is, of course, exactly Gaussian at all times. In Durbin's model (not shown) p_Σ is also close to Gaussian (Sawford 1983). A Gaussian shape for p_Σ is to be expected at small times (as a consequence of the assumed Gaussianity of the fixed-point velocity distribution) and at large times (on the basis of a central limit theorem type argument) and so the observed Gaussianity is not surprising.

Figure 3 shows the growth of σ_1, σ_Δ and σ_Σ in the new model and in the NGLS model. At small times σ_1 and σ_Σ are proportional to $t-s$ (as is to be expected since the particle trajectories can be approximated by straight lines over short times) while σ_Δ grows like $(t-s)^{\frac{3}{2}}$ (as is expected on dimensional grounds – see e.g. Monin & Yaglom 1975, p. 545). At large $t-s$, σ_1, σ_Δ and σ_Σ grow like $(t-s)^{\frac{1}{2}}$. The $(t-s)^{\frac{1}{2}}$ growth

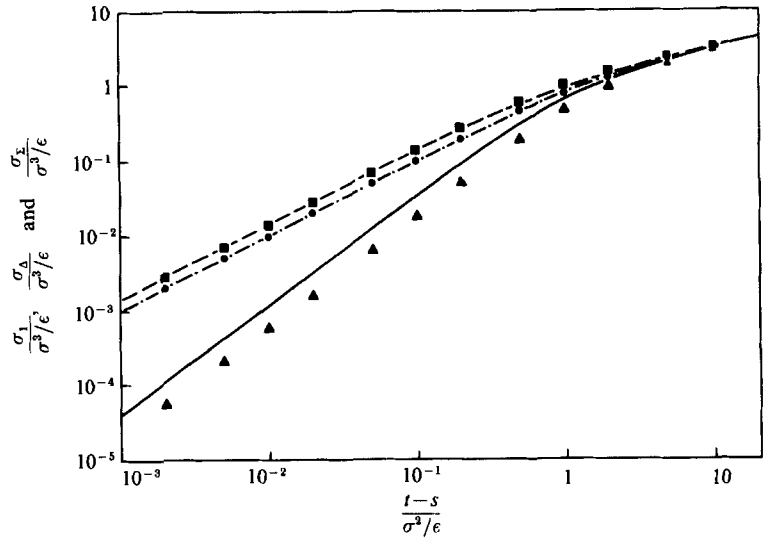

FIGURE 3. $\sigma_1(t\,|\,s)$, $\sigma_\Delta(t\,|\,s)$ and $\sigma_\Sigma(t\,|\,s)$ in stationary turbulence. The values of σ_1, σ_Δ and σ_Σ obtained from the new model are denoted by ●, ▲ and ■, and the values obtained from the NGLS model are indicated by —·—, —— and – – –.

of σ_1 is expected on the basis of Taylor's (1921) result. Also σ_Δ and σ_Σ are expected to grow in the same way as σ_1 at large $t-s$ since, at large $t-s$, the particle pairs will have spent most of their time at large separations where they travel independently. The values of σ_1, σ_Δ and σ_Σ from the NGLS model can be obtained analytically and are as follows:

$$\sigma_1^2(t\,|\,s) = 2\sigma^2\tau^2(\exp(-(t-s)/\tau)-1+(t-s)/\tau),$$
$$\sigma_\Delta^2(t\,|\,s) = \sigma_1^2-\sigma^2\tau^2(1-\exp(-(t-s)/\tau))^2,$$
$$\sigma_\Sigma^2(t\,|\,s) = \sigma_1^2+\sigma^2\tau^2(1-\exp(-(t-s)/\tau))^2.$$

In the new model, the value of σ_1 is indistinguishable from that in the NGLS model. This is as it should be if (21) is not to be seriously violated. This is because, for large initial separation (with $\boldsymbol{x}_1(s) = 0$),

$$\overline{(x_1^1)^2} = \overline{(x_1^2)^2} = \overline{(x_1^3)^2} = 2\sigma^2\tau^2(\exp(-(t-s)/\tau)-1+(t-s)/\tau)$$

in the new model (this follows from (19)) and these quantities should be independent of initial separation since they depend on the motion of one particle only. The value of σ_Δ in the new model is smaller than the value from the NGLS model. This is to be expected because, if the particles in the new model approach closely at some time after release, their velocities become highly correlated again, reducing the rate of growth of σ_Δ.

In order to see how seriously the new model violates (21), the mean and root-mean-square values of the various components of $\boldsymbol{x}_1$ were calculated for a range of initial separations. These quantities should be independent of $\Delta(s)$ if (21) is to be satisfied. It was found that this is indeed the case, with the root-mean-square values all lying within a few per cent of each other and the mean values all equalling zero to an accuracy of a few per cent of the root-mean-square value. In addition $\overline{U^iU^i}$ was calculated for various initial separations. The values of $\overline{U^iU^i}$ do not show any strong dependence on the initial separation and equal $6\sigma^2$ to within a few per cent. This lends further support to the idea that the violation of (21) may not be too severe, and

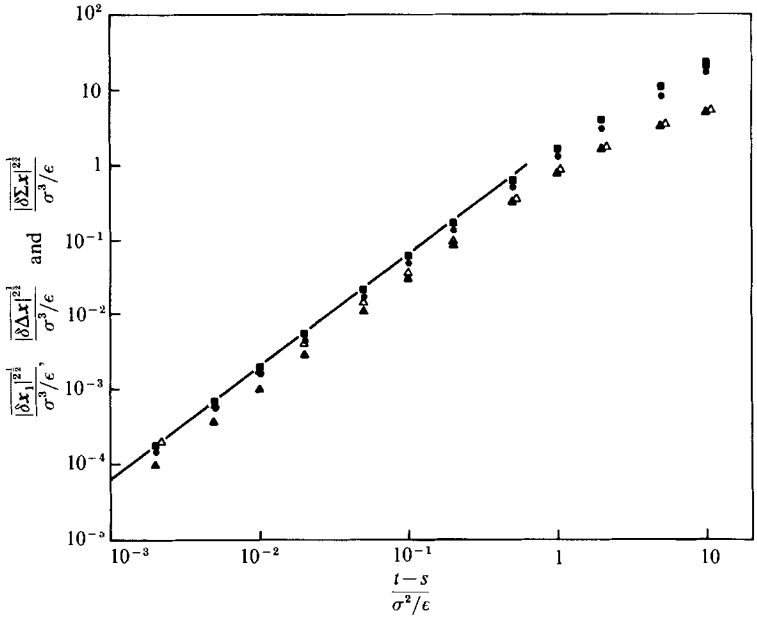

FIGURE 4. $\overline{|\delta x_1|^2}$, $\overline{|\delta\Delta x|^2}$ and $\overline{|\delta\Sigma x|^2}$ from the new model for particle pairs released at time s in stationary turbulence. ●, ▲ and ■ denote $\overline{|\delta x_1|^2}$, $\overline{|\delta\Delta x|^2}$ and $\overline{|\delta\Sigma x|^2}$ respectively for zero initial separation. △ denotes $\overline{|\delta\Delta x|^2}$ for an initial separation of $2\times10^{-3}l$. The solid line is $C_0\epsilon t^3$.

suggests that either the higher-order terms in (23) have a corrective effect or the power series expansion ceases to be applicable after a short time. We also note that the distribution of $\boldsymbol{x}_1$ in the model is Gaussian for large initial separations (this follows from (19)) and hence that it should be close to Gaussian for all initial separations if (21) is to be approximately true. The simulations indicate that this is in fact the case, with the p.d.f.s of $\boldsymbol{x}_1$ for various initial separations and travel times (not shown) having a degree of scatter about a Gaussian distribution similar to that seen in figure 2.

There is however one aspect of the new model which violates (21) significantly. Consider the quantity $\delta\boldsymbol{x}_1(t) = \boldsymbol{x}_1(t) - \boldsymbol{x}_1(s) - \boldsymbol{u}_1(s)\,(t-s)$. For $t-s \ll \tau$, $\overline{|\delta\boldsymbol{x}_1|^2}$ should grow like $C_0\epsilon(t-s)^3$, the value which $\overline{|\delta\boldsymbol{x}_1|^2}$ takes when $\Delta(s) \gg l$ (this follows from (19)). As in (22), the average here is over particle pairs with a given position in $\boldsymbol{X}$-space at time s. For $\Delta(s) = 0$, the value of $\overline{|\delta\boldsymbol{x}_1|^2}$ from the model is significantly smaller than $C_0\epsilon(t-s)^3$ (see figure 4). Some insight into why this is so can be obtained by considering $\delta\Delta\boldsymbol{x}$ and $\delta\Sigma\boldsymbol{x}$, defined in a way analogous to $\delta\boldsymbol{x}_1$. It is easy to show that $|\delta\boldsymbol{x}_1|^2 + |\delta\boldsymbol{x}_2|^2 = |\delta\Delta\boldsymbol{x}|^2 + |\delta\Sigma\boldsymbol{x}|^2$ and so, by symmetry, $\overline{|\delta\boldsymbol{x}_1|^2} = \frac{1}{2}(\overline{|\delta\Delta\boldsymbol{x}|^2} + \overline{|\delta\Sigma\boldsymbol{x}|^2})$. Hence, for $t-s \ll \tau$,

$$\tfrac{1}{2}(\overline{|\delta\Delta\boldsymbol{x}|^2} + \overline{|\delta\Sigma\boldsymbol{x}|^2}) = C_0\,\epsilon(t-s)^3 \tag{26}$$

should hold. In the model the leading-order term in the Taylor series for $\overline{|\delta\Delta\boldsymbol{x}|^2}$ and $\overline{|\delta\Sigma\boldsymbol{x}|^2}$ is $C_0\epsilon(t-s)^3$ and so (26) is satisfied at small times. If $\Delta(s) \ll l$, then, while $\Delta \ll l$ (i.e. for $t-s \ll \tau$), the stochastic differential equations for $\delta\Sigma\boldsymbol{x}$ and $\delta\Sigma\boldsymbol{u}(t) = \Sigma\boldsymbol{u}(t) - \Sigma\boldsymbol{u}(s)$ can be approximated by

$$\mathrm{d}\delta\Sigma\boldsymbol{x} = \delta\Sigma\boldsymbol{u}\,\mathrm{d}t, \quad \mathrm{d}\delta\Sigma\boldsymbol{u} = (C_0\epsilon)^{\frac{1}{2}}\mathrm{d}\boldsymbol{\xi},$$

with $\delta\Sigma\boldsymbol{u}(s) = 0$ (the terms which have been omitted in this approximation have an effect which is only significant over timescales of order τ). Hence $\overline{|\delta\Sigma\boldsymbol{x}|^2} = C_0\epsilon(t-s)^3$

for $t-s \ll \tau$. However the equations for $\delta\Delta\boldsymbol{x}$ and $\delta\Delta\boldsymbol{u} = \Delta\boldsymbol{u}(t) - \Delta\boldsymbol{u}(s)$ are much more complex and, in addition to a $(C_0\epsilon)^{\frac{1}{2}}\mathrm{d}\boldsymbol{\xi}$ term, the expression for $\mathrm{d}\delta\Delta\boldsymbol{u}$ contains terms which, for particle separations lying in the inertial subrange, are of order $(\epsilon^2/\Delta)^{\frac{1}{3}}\mathrm{d}t$. Over a time of order $(\Delta^2/\epsilon)^{\frac{1}{3}}$ these terms have an effect comparable to the effect of the $(C_0\epsilon)^{\frac{1}{2}}\mathrm{d}\boldsymbol{\xi}$ term. Hence $\overline{|\delta\Delta\boldsymbol{x}|^2} \approx C_0\epsilon(t-s)^3$ only holds for $t-s \ll (\Delta(s)^2/\epsilon)^{\frac{1}{3}}$. For $(\Delta(s)^2/\epsilon)^{\frac{1}{3}} \ll t-s \ll \tau$, $\overline{|\delta\Delta\boldsymbol{x}|^2}$ grows like $(t-s)^3$ but with a different coefficient. This difference in the coefficient of $(t-s)^3$ for $t-s \ll (\Delta(s)^2/\epsilon)^{\frac{1}{3}}$ and for

$$(\Delta(s)^2/\epsilon)^{\frac{1}{3}} \ll t-s \ll \tau$$

is clearly seen in the results obtained with an initial separation of $2\times10^{-3}l$ (figure 4). For this value of the initial separation, the 'cross-over' time $(\Delta(s)^2/\epsilon)^{\frac{1}{3}}$ equals $10^{-2}\sigma^2/\epsilon$.

Consider a pair of particles whose initial separation lies well within the inertial subrange and consider their motions over times for which the evolution of $\delta\boldsymbol{x}_1$ and $\delta\Delta\boldsymbol{x}$ is dominated by inertial subrange eddies. In the model, for which the inertial subrange extends to arbitrarily high wavenumbers and frequencies, this means restricting attention to initial separations with $\Delta(s) \ll l$ and travel times satisfying $t-s \ll \tau$. By assuming that the covariance between the accelerations of two particles whose separation lies in the inertial subrange is negligible, Monin & Yaglom (1975, pp. 546–547) and Sawford (1984) deduce that $\overline{|\delta\boldsymbol{x}_1|^2} = \overline{|\delta\Delta\boldsymbol{x}|^2}$ for such initial separations and travel times. (Monin & Yaglom (1975) and Sawford (1984) were principally concerned with the case where the initial separation is zero or where the initial separation is non-zero and the travel time is sufficiently large for the particles to forget their initial separation. In this case $\overline{|\delta\Delta\boldsymbol{x}|^2}$ equals the mean square separation $\overline{|\Delta\boldsymbol{x}|^2}$. However their analysis applies more generally.) If this is true it follows that the value of $\overline{|\delta\Delta\boldsymbol{x}|^2}$ in the model is incorrect for times in the range $(\Delta(s)^2/\epsilon)^{\frac{1}{3}} \ll t-s \ll \tau$. However the argument in Appendix B shows that the inertial subrange acceleration covariances may be important in reality (they certainly are in the model since, as we have noted, the model value of $\overline{|\delta\boldsymbol{x}_1|^2}$ is greater than $\overline{|\delta\Delta\boldsymbol{x}|^2}$ for $(\Delta(s)^2/\epsilon)^{\frac{1}{3}} \ll t-s \ll \tau$), and that it is more likely that $\overline{|\delta\boldsymbol{x}_1|^2}$ is, in reality, greater than $\overline{|\delta\Delta\boldsymbol{x}|^2}$ for times in the range $(\Delta(s)^2/\epsilon)^{\frac{1}{3}} \ll t-s \ll \tau$. Hence the model value of $\overline{|\delta\Delta\boldsymbol{x}|^2}$ is not unreasonable and the cause of the problem could be the model's value for $\overline{|\delta\Sigma\boldsymbol{x}|^2}$.

It is not clear if the above problem is a serious flaw in the model. However it should be pointed out that this flaw is not one which is apparent in the single-time statistics of particle pairs whose trajectories commence at a given position in $\boldsymbol{X}$-space. The single-time statistics, at least as judged by the evidence presented earlier in this section, show little evidence of violation of (21). For many purposes, in particular for predicting concentration fluctuations in the situations which will be considered in §6, it is only the single-time statistics which are important. This suggests that the violation of (21) may not matter in practice.

5.2. *Decaying turbulence*

A number of simulations were also carried out in decaying isotropic turbulence. The velocity field was assumed to decay self-similarly with σ^2 varying as $\sigma_s^2(t/s)^{-n}$ where σ_s is the value of σ at time s. The value of n was taken to be 1.35, which is within the scatter of values observed in grid turbulence (Warhaft 1984; Warhaft & Lumley 1978). Of course the decay exponent measured in grid turbulence is the exponent for the decay of σ^2 with downwind distance in a steady inhomogeneous flow. However, it can be interpreted as the exponent for the decay in time of isotropic turbulence in

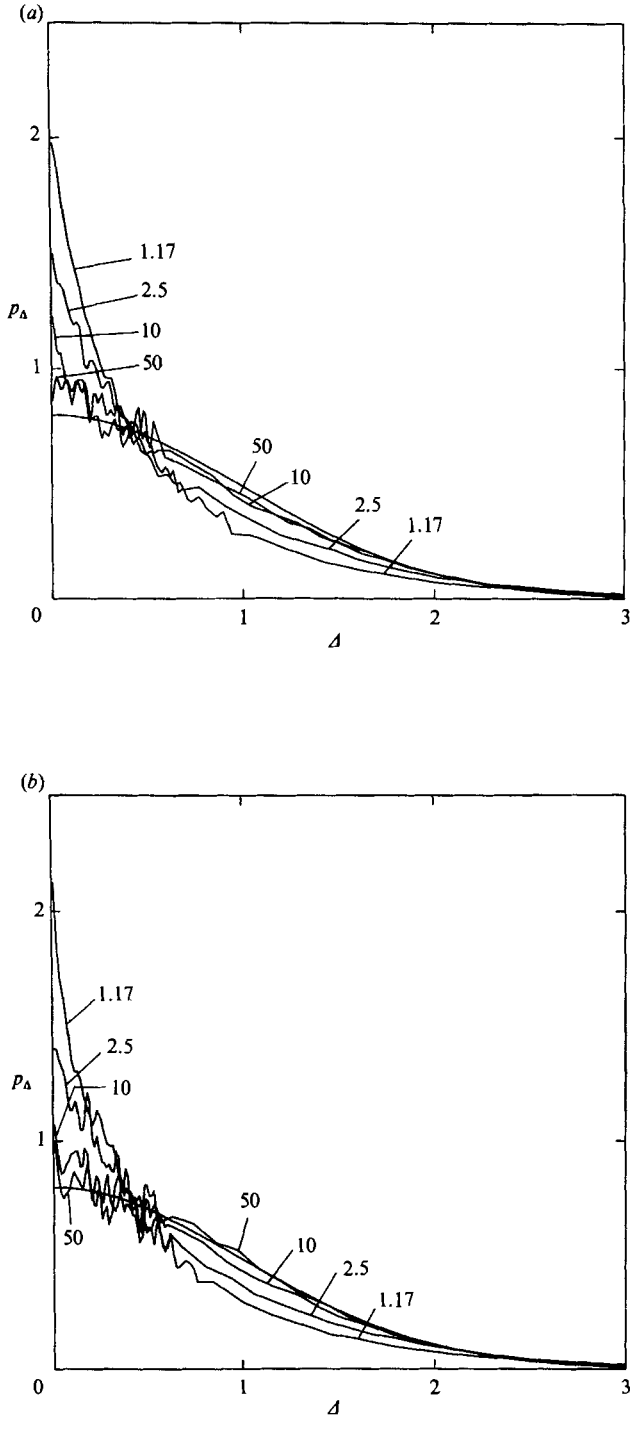

FIGURE 5. The shape of $p_\Delta(\Delta, t|s)$ from the new model in decaying turbulence. The curves were obtained using the particle-splitting technique and are normalized with zeroth and second moments equal to unity as if they were one-dimensional p.d.f.s (*a*) shows results for $t > s$ (forward trajectories) and (*b*) shows results for $t < s$ (backwards trajectories). The numbers attached to the curves indicate values of t/s for the forward trajectories and s/t for the backwards trajectories. In both figures the unlabelled line is a Gaussian distribution.

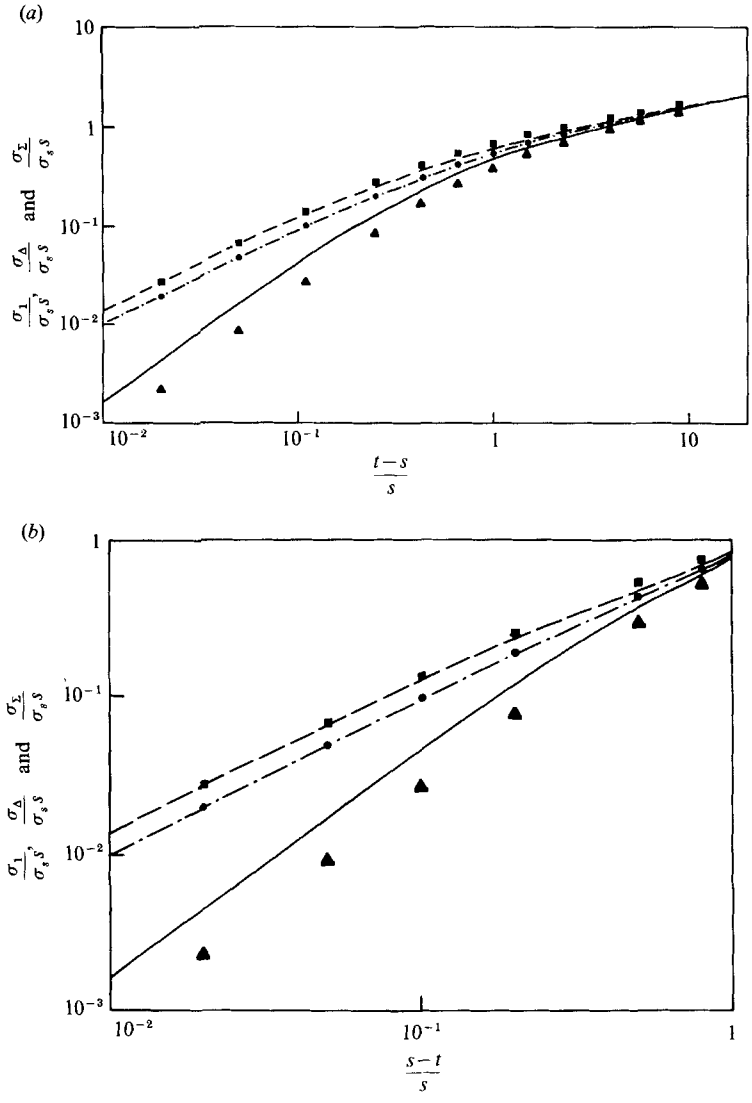

FIGURE 6. $\sigma_1(t|s)$, $\sigma_\Delta(t|s)$ and $\sigma_\Sigma(t|s)$ in decaying turbulence. The values of σ_1, σ_Δ and σ_Σ obtained from the new model are denoted by ●, ▲ and ■, and the values obtained from the NGLS model are indicated by —·—, —— and – – –. (*a*) shows results for $t > s$ (forward trajectories) and (*b*) shows results for $t < s$ (backwards trajectories).

the usual way (Monin & Yaglom 1975, pp. 115–116). With this form for σ^2, ϵ is equal to $1.5n(\sigma_s^2/s)\,(t/s)^{-(n+1)}$, which, assuming the relation between σ^2, ϵ and l given in §4.1, implies $l = (\sqrt{2/3n})\,\sigma_s\, s(t/s)^{1-\frac{1}{2}n}$.

Trajectories of particle pairs were simulated both forward and backwards in time, the particles being coincident at the time of release. The same release time was used in all the simulations. Because the turbulence decays self-similarly, the results can be rescaled (Durbin 1982) to give results for other release times, for example

$$p_2(\boldsymbol{x}_1, \boldsymbol{x}_2, t, t\,|\,0, 0, s, s) = \gamma^{6-3n} p_2(\boldsymbol{x}_1 \gamma^{1-\frac{1}{2}n}, \boldsymbol{x}_2 \gamma^{1-\frac{1}{2}n}, \gamma t, \gamma t\,|\,0, 0, \gamma s, \gamma s) \qquad (27)$$

for any $\gamma > 0$.

The shape of p_Δ is shown in figure 5. Because of the scaling relation (27), the shape

of p_Δ depends only on t/s. The shape becomes quite close to Gaussian as $t/s \to 0$; however there is some indication that the shape remains more peaked than a Gaussian distribution as $t/s \to \infty$. Figure 6 shows the values of σ_1, σ_Δ and σ_Σ from the new model and from the NGLS model. As is to be expected, the behaviour of σ_1, σ_Δ and σ_Σ for small $|t-s|$ is the same as in the stationary case. For the forward trajectories, σ_1, σ_Δ and σ_Σ become, at large times, proportional to $(t-s)^{1-\frac{1}{2}n}$. This form of large-time behaviour is expected both on dimensional grounds and from consideration of a modified version of Taylor's (1921) result (see Batchelor & Townsend (1956) and Monin & Yaglom (1971, §9.4) for a discussion of the case $n = 1$). The values from the NGLS model can be obtained analytically and are

$$\sigma_1^2(t\,|\,s) = 2\sigma_s^2 s^2\left(\frac{(t/s)^{r-q}-1}{r(r-q)} + \frac{(t/s)^{-q}-1}{rq}\right),$$

$$\sigma_\Delta^2(t\,|s) = \sigma_1^2 - \sigma_s^2 s^2\left(\frac{(t/s)^{-q}-1}{q}\right)^2,$$

$$\sigma_\Sigma^2(t\,|s) = \sigma_1^2 + \sigma_s^2 s^2\left(\frac{(t/s)^{-q}-1}{q}\right)^2,$$

where $r = \alpha - \frac{1}{2}n + 1$, $q = \alpha + \frac{1}{2}n - 1$ for the forward trajectories ($t > s$) and $r = -\alpha - \frac{1}{2}n + 1$, $q = -\alpha + \frac{1}{2}n - 1$ for the reverse trajectories ($t < s$), with $\alpha = \frac{3}{4}nC_0$ (Anand & Pope 1985). As in the stationary case the value of σ_Δ in the new model is considerably smaller than the value from the NGLS model, while the values of σ_1 in the two models are indistinguishable. The close agreement between the values of σ_1 lend support, as in the stationary case, to the idea that (21) is not seriously violated. The homogeneity of the flow and equation (7) imply that, in reality, $\sigma_1(t\,|\,s) = \sigma_1(s\,|\,t)$. This is satisfied exactly in the NGLS model and to high accuracy in the new model. It is of interest that the values of $\sigma_1(t\,|\,s)/\sigma_\Delta(t\,|\,s)$ and $\sigma_1(t\,|\,s)/\sigma_\Sigma(t\,|\,s)$ for the backward trajectories do not tend to unity as $t/s \to 0$ while the values for the forward trajectories do tend to unity as $t/s \to \infty$. A consequence of this is that $\sigma_\Delta(t\,|\,s) > \sigma_\Delta(s\,|\,t)$ in the limit $t/s \to \infty$, while, as a result of (8), $p_\Delta(0, s\,|\,t) = p_\Delta(0, t\,|\,s)$. It follows that the shape of $p_\Delta(\Delta, t\,|\,s)$ must be more peaked in the limit $t/s \to \infty$ than in the limit $t/s \to 0$, as is observed in figure 5 (note this argument does not apply to the NGLS model which does not satisfy (8) because of the inconsistency noted in §4.2 between the initial conditions on the particle velocities and the form of g_a with which the model is consistent). It will be seen below that this has implications for the intensity of concentration fluctuations at large times.

6. Concentration variances from the model

In this section values of concentration variance $\sigma_c^2 = \langle c^2\rangle - \langle c\rangle^2$ from the new model are presented and some comparisons with experimental data are made. Only deterministic instantaneous sources are considered and the release time will be denoted by s. For $t > s$, the reverse dispersion relations given in §2 can then be written as

$$\langle c(\boldsymbol{x}, t)\rangle = \int p_1(\boldsymbol{y}, s\,|\,\boldsymbol{x}, t)\, S(\boldsymbol{y})\, \mathrm{d}\boldsymbol{y} \tag{28}$$

and

$$\langle c(\boldsymbol{x}, t)^2\rangle = \int p_2(\boldsymbol{y}_1, \boldsymbol{y}_2, s, s\,|\,\boldsymbol{x}, \boldsymbol{x}, t, t)\, S(\boldsymbol{y}_1)\, S(\boldsymbol{y}_2)\, \mathrm{d}\boldsymbol{y}_1\, \mathrm{d}\boldsymbol{y}_2, \tag{29}$$

where $S(\boldsymbol{x})$ is the source strength (as in §5, S here has a slightly different meaning to the S introduced in §2, being the amount of tracer released per unit volume, not per

unit space–time volume). It is useful to apply an approximation intoduced by Sawford (1983) and replace p_1 in (28) by

$$G_3(\boldsymbol{y}-\boldsymbol{x}, \sigma_1^2(s\,|\,t)), \tag{30}$$

and p_2 in (29) by $$p_\Delta(\Delta\boldsymbol{y}, s\,|\,t)\, G_3(\Sigma\boldsymbol{y}-\boldsymbol{x}\sqrt{2}, \sigma_\Sigma^2(s\,|\,t)), \tag{31}$$

where $\Delta\boldsymbol{y} = (\boldsymbol{y}_1-\boldsymbol{y}_2)/\sqrt{2}$, $\Sigma\boldsymbol{y} = (\boldsymbol{y}_1+\boldsymbol{y}_2)/\sqrt{2}$ and $G_\lambda(\boldsymbol{x}, \sigma^2)$ denotes a λ-dimensional Gaussian distribution with variance σ^2, i.e.

$$G_3(\boldsymbol{x}, \sigma^2) = \frac{1}{(2\pi)^{\frac{3}{2}}\sigma^3}\exp(-|\boldsymbol{x}|^2/2\sigma^2),$$

$$G_2(\boldsymbol{x}, \sigma^2) = \frac{1}{2\pi\sigma^2}\exp(-((x^2)^2+(x^3)^2)/2\sigma^2),$$

$$G_1(\boldsymbol{x}, \sigma^2) = \frac{1}{(2\pi)^{\frac{1}{2}}\sigma}\exp(-(x^3)^2/2\sigma^2).$$

The assumptions involved here are that the distribution of $\boldsymbol{x}$ and $\Sigma\boldsymbol{x}$ are approximately Gaussian (which is true) and that, for particle pairs with separation zero at time s, $\Delta\boldsymbol{x}$ and $\Sigma\boldsymbol{x}$ are approximately independent. The latter assumption is hard to verify directly but appears reasonable because of the weak dependence of $\mathrm{d}\Sigma\boldsymbol{x}$ on $\Delta\boldsymbol{x}$, the absence of any dependence of $\mathrm{d}\Delta\boldsymbol{x}$ on $\Sigma\boldsymbol{x}$, and the fact that the covariance of $\Delta\boldsymbol{x}$ and $\Sigma\boldsymbol{x}$ is zero. A comparison presented below between values of σ_c obtained with and without this approximation gives some indirect support for the assumption. The advantages of using the approximations (30) and (31) are that it reduces statistical noise and makes it easier to see how the different aspects of p_1 and p_2 (e.g. σ_1, σ_Δ, σ_Σ, shape of p_Δ) influence σ_c.

Calculations of $\langle c^2\rangle$ and $\langle c\rangle$ were carried out for area, line and compact sources centred on the origin. The source size will be denoted by σ_0. The source is taken to be Gaussian, i.e. $S(\boldsymbol{x}) = G_\lambda(\boldsymbol{x}, \sigma_0^2)$ where λ is 1 for an area source, 2 for a line source and 3 for a compact source. As discussed by Sawford (1983), $\langle c\rangle$ and $\langle c^2\rangle$ are, with the approximations (30) and (31), given by

$$\langle c(\boldsymbol{x}, t)\rangle = G_\lambda(\boldsymbol{x}, \sigma_1^2(s\,|\,t)+\sigma_0^2) \tag{32}$$

and $$\langle c(\boldsymbol{x}, t)^2\rangle = \int p_\Delta(\Delta\boldsymbol{y}, s\,|\,t)\, G_\lambda(\Delta\boldsymbol{y}, \sigma_0^2)\,\mathrm{d}\Delta\boldsymbol{y}\, G_\lambda(\boldsymbol{x}\sqrt{2}, \sigma_\Sigma^2(s\,|\,t)+\sigma_0^2). \tag{33}$$

Some calculations will also be presented for two parallel Gaussian areas sources. For this situation expressions analogous to (32) and (33) can be easily derived.

6.1. *Stationary turbulence*

Figures 7 (*a*), 7 (*b*) and 7 (*c*) show values of $\sigma_c/\langle c\rangle$ at $\boldsymbol{x} = 0$ for area, line and compact sources of various sizes. Some statistical noise is evident at small values of $\sigma_c/\langle c\rangle$, especially at large times. This is because, when $\sigma_c/\langle c\rangle$ is small, small errors in $\langle c^2\rangle$ and $\langle c\rangle$ can result in a large error in σ_c. The results show clearly the strong effect which source size has near the source and suggest that $\sigma_c/\langle c\rangle$ becomes independent of source size and tends to zero at large time. Because of statistical noise, it is impossible, in the absence of an analytic solution to the model, to state with certainty that $\sigma_c/\langle c\rangle$ tends to zero. However, if $p_\Delta(\Delta, s\,|\,t)$ is exactly Gaussian at large t, then (32) and (33) imply

$$\frac{\sigma_c}{\langle c\rangle} = \left(\frac{(\sigma_1^2(s\,|\,t)+\sigma_0^2)^\lambda}{((\sigma_\Delta^2(s\,|\,t)+\sigma_0^2)\,(\sigma_\Sigma^2(s\,|\,t)+\sigma_0^2))^{\frac{1}{2}\lambda}}-1\right)^{\frac{1}{2}} \tag{34}$$

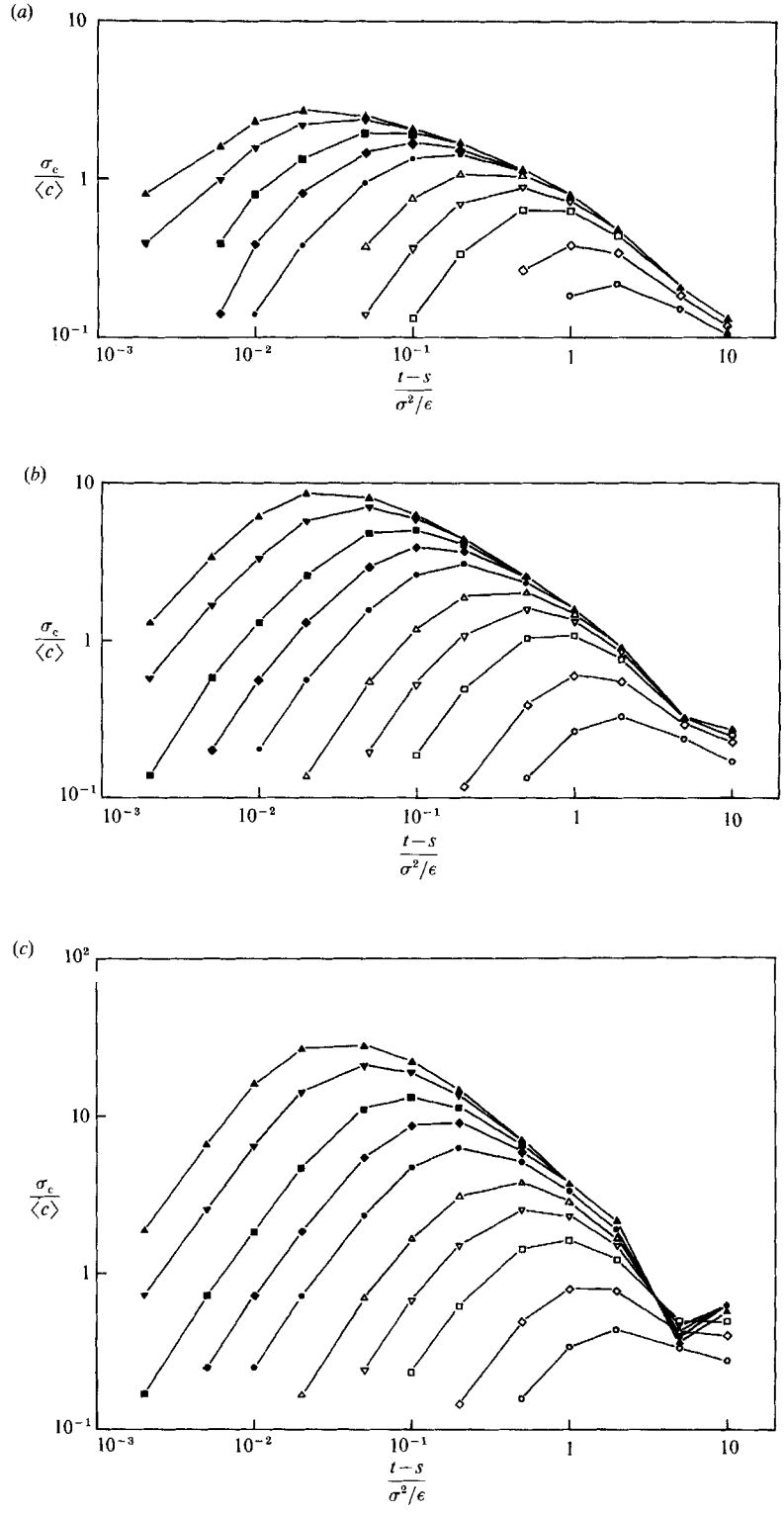

FIGURE 7 (*a–c*). For caption see facing page.

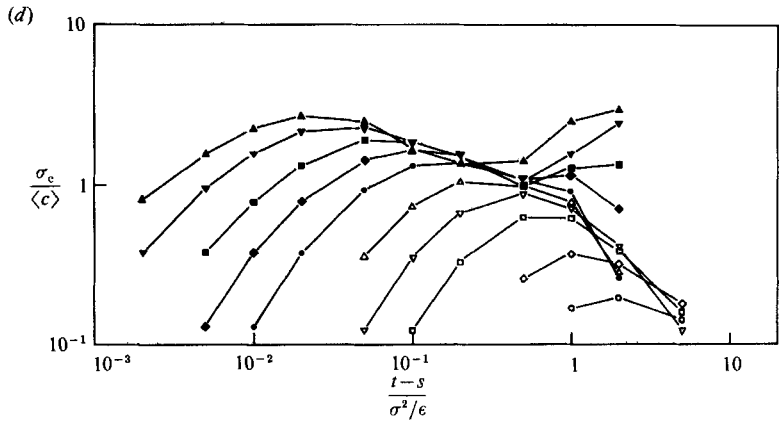

FIGURE 7. Values of $\sigma_c/\langle c \rangle$ at $x = 0$ from the model in stationary conditions. (*a*) shows results for an area source, (*b*) for a line source and (*c*) for a compact source. (*d*) shows results for an area source calculated without using the approximation (31). The different symbols refer to different source sizes: ▲, $\sigma_0 = 0.001\sigma^3/\epsilon$; ▼, $\sigma_0 = 0.002\sigma^3/\epsilon$; ■, $\sigma_0 = 0.005\sigma^3/\epsilon$; ◆, $\sigma_0 = 0.01\sigma^3/\epsilon$; ●, $\sigma_0 = 0.02\sigma^3/\epsilon$; △, $\sigma_0 = 0.05\sigma^3/\epsilon$; ▽, $\sigma_0 = 0.1\sigma^3/\epsilon$; □, $\sigma_0 = 0.2\sigma^3/\epsilon$; ◇, $\sigma_0 = 0.5\sigma^3/\epsilon$; ○, $\sigma_0 = \sigma^3/\epsilon$.

at large times. Hence, because $\sigma_1(s\,|\,t)/\sigma_A(s\,|\,t)$ and $\sigma_1(s\,|\,t)/\sigma_\Sigma(s\,|\,t)$ tend to unity as $t \to \infty$, $\sigma_c/\langle c \rangle \to 0$ at large times.

Values of $\sigma_c/\langle c \rangle$ for an area source, obtained without using the approximation (31) (but still using (30)) are shown in figure 7(*d*). In evaluating (29), p_2 was represented as a sum of a number of delta functions located at the positions of the particle pairs in the simulation. At small times the results show good agreement with the results obtained using (31) (figure 7*a*), lending support to the assumption that Δx and Σx are approximately independent. At larger times however the scatter becomes very great due to the small number of particle pairs passing through the source. For example, for small sources at large times the expected number of particle pairs passing through the source can be less than one. In this situation either no particle pairs pass through and the calculated value of $\langle c^2 \rangle$ is zero, or one or more particle pairs pass through and $\sigma_c/\langle c \rangle$ is large. It may be possible to improve matters by smoothing p_2 and by the use of a suitable form of particle splitting to ensure that there are always a lot of particle pairs near the source; however this has not been attemped here. For line and compact sources (not shown) the scatter is even greater.

Figure 8 shows a comparison between the model results and the experimental wind-tunnel data of Fackrell & Robins (1982). In the wind-tunnel experiments material was released into a turbulent boundary layer from a continuous compact elevated source. For comparison with the model, the experimental data obtained at a distance x downwind of the source is regarded as data obtained at time x/U after the release of an instantaneous line source in stationary isotropic turbulence (here U denotes the mean velocity at the source in the experiments). Provided the anisotropy of the flow can be neglected, this should be a good approximation; this is because the intensity of turbulence in the experiments was small (see e.g. Townsend (1954), Anand & Pope (1985) or Sawford & Hunt (1986) for a discussion of a similar approximation – the approximation of a continuous line source by an instantaneous area source). The wind-tunnel results are of course affected by the shear and the inhomogeneity in the flow and the anisotropy of the (one-point) velocity covariance tensor; however the effect of the shear and inhomogeneity should be unimportant for

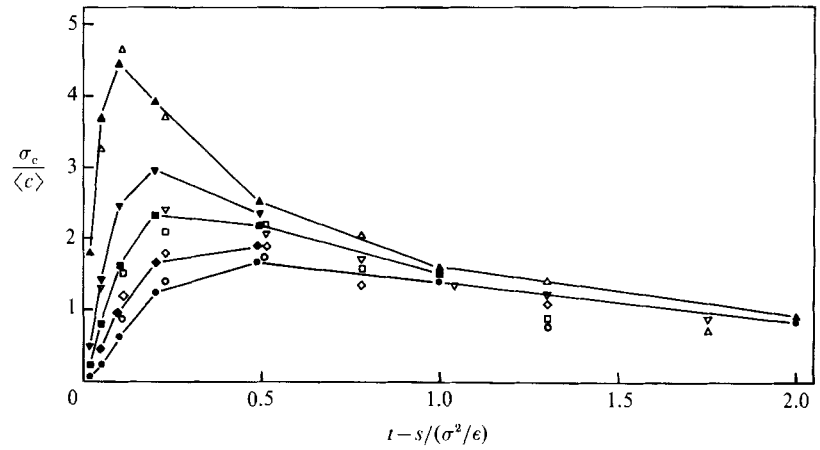

FIGURE 8. Comparison of $\sigma_c/\langle c \rangle$ at $x = 0$ from the model with the experimental data of Fackrell & Robins (1982). Model results are indicated by solid symbols and experimental results by open symbols. The different symbol shapes refer to different source sizes: ▲, $\sigma_0 = 7.41 \times 10^{-3}\sigma^3/\epsilon$; ▼, $\sigma_0 = 2.22 \times 10^{-2}\sigma^3/\epsilon$; ■, $\sigma_0 = 3.7 \times 10^{-2}\sigma^3/\epsilon$; ◆, $\sigma_0 = 6.17 \times 10^{-2}\sigma^3/\epsilon$; ●, $\sigma_0 = 8.64 \times 10^{-2}\sigma^3/\epsilon$.

travel times less than about $0.5\sigma^2/\epsilon$, the time at which the tracer first reaches the ground in significant quantities. In contrast the anisotropy of the velocity covariance tensor is likely to have some effect on the results, but, because the anisotropy is not large, the effect is unlikely to be of major importance. In plotting the experimental results in figure 8, σ^2 was taken to be the average of the velocity variances in three orthogonal directions. The agreement between the model and experimental results is good although, because of the uncertainty in the universal constant C_0 and the arbitrary way in which f was chosen (equation (16)), this may be partly fortuitous. It is somewhat surprising that the agreement remains good for $t-s > 0.5\sigma^2/\epsilon$ when the effect of shear and inhomogeneity might be expected to be significant. The observed and modelled behaviour is different to the type of behaviour seen in Durbin's model where $\sigma_c/\langle c \rangle$ increases monotonically to an asymptotic value.

Figure 9 shows examples of profiles of σ_c for a line source with σ_0 equal to $2.22 \times 10^{-2}\sigma^3/\epsilon$, the source size used in most of Fackrell & Robins' experiments. As time increases the profile evolves through three stages. At first the σ_c profile has its peak away from the origin at the point where the gradient of $\langle c \rangle$ is greatest. As time advances the peak moves towards the origin and, in what will be referred to as the second stage, the peak is at $x = 0$. This stage lasts from $t-s = 0.05\sigma^2/\epsilon$ to $t-s = 2\sigma^2/\epsilon$. In the third and final stage, the off-centre peak reappears. At all times the σ_c profile is somewhat wider than the profile of the mean concentration. Similar behaviour is observed for other small source sizes, although the time of transition between the first and second stages increases with source size. For large sources, with σ_0 comparable to σ^3/ϵ, the behaviour is somewhat different, the first stage lasting so long that it merges into the third stage with the second stage being squeezed out of existence. For area sources the second stage begins later and ends earlier while the reverse is true for compact sources. In the case of compact sources the evidence for the reappearance of the off-centre peak is not so clear cut, the peak appearing and disappearing repeatedly at large times due to the statistical scatter discussed above. The first stage in the evolution of σ_c is to be expected because, at small times after

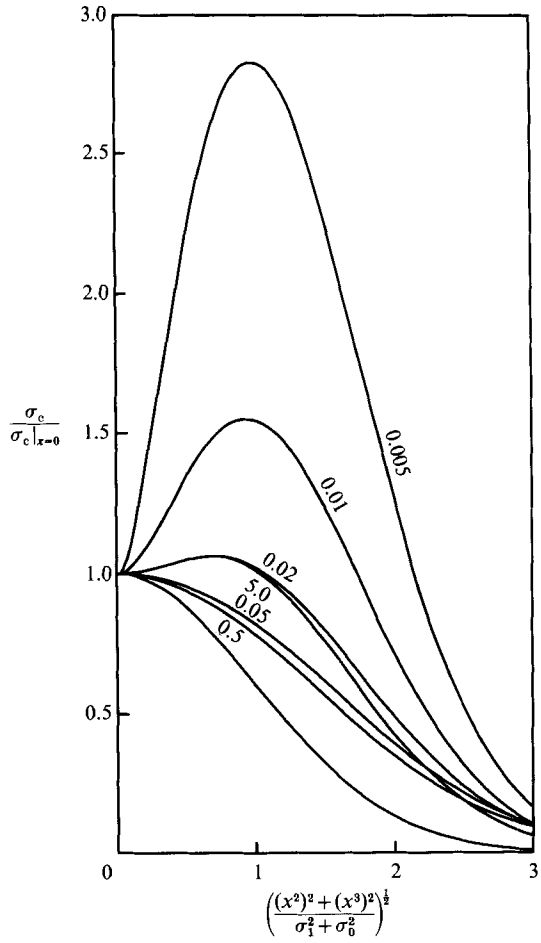

FIGURE 9. Profiles of σ_c from the model for a line source in stationary conditions. $\sigma_0 = 2.22 \times 10^{-2}\sigma^3/\epsilon$. The numbers attached to the curves indicate values of $t-s$ normalized by σ^2/ϵ. The unlabelled curve is a Gaussian distribution with the same standard deviation as the profile of $\langle c \rangle$.

release, the fluctuations arise directly from the local gradients of mean concentration. Some understanding of the second stage can be obtained by considering (32) and (33). These equations imply that the peak will occur off the centreline when

$$\frac{\langle c(0,t)^2 \rangle}{\langle c(0,t) \rangle^2} \frac{\sigma_1^2(s\,|\,t)+\sigma_0^2}{\sigma_\Sigma^2(s\,|\,t)+\sigma_0^2} < 1; \tag{35}$$

in particular, since $\sigma_\Sigma^2 \leqslant 2\sigma_1^2$, the peak must be on the centreline when $\sigma_c/\langle c \rangle \geqslant 1$. At large times p_Δ becomes close to Gaussian. If p_Δ is exactly Gaussian, then (32), (33) and the fact that $\sigma_1(s\,|\,t)/\sigma_\Delta(s\,|\,t)$ and $\sigma_1(s\,|\,t)/\sigma_\Sigma(s\,|\,t)$ tend to unity at large t imply that the left-hand side of (35) is less than 1 at large t (and approaches 1 as $t \to \infty$) and so explains the reappearance of the peak in the third stage. The reappearance of the off-centre peak suggests that at large times σ_c is again partly determined by local processes, with σ_c peaking in the vicinity of the point where the production of concentration variance from the local mean concentration gradient is a maximum.

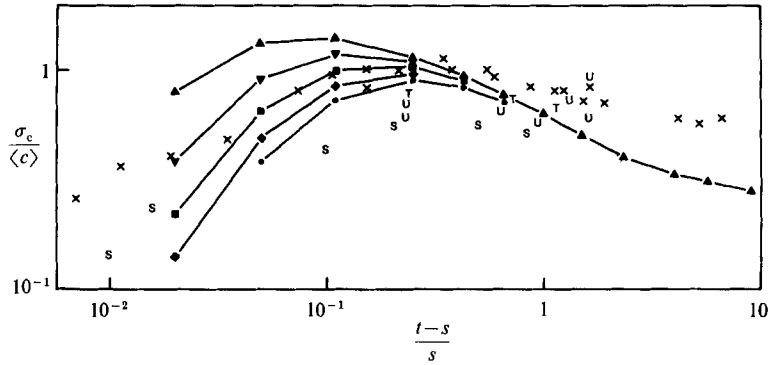

FIGURE 10. Comparison of $\sigma_c/\langle c \rangle$ at $x = 0$ from the model with the experimental data of Warhaft (1984). The model results for various source sizes are indicated by the following symbols: ▲, $\sigma_0 = 0.01\sigma_s s$; ▼, $\sigma_0 = 0.02\sigma_s s$; ■, $\sigma_0 = 0.03\sigma_s s$; ◆, $\sigma_0 = 0.04\sigma_s s$; ●, $\sigma_0 = 0.05\sigma_s s$. The experimental results of Warhaft (1984) are denoted by crosses. Also shown are the experimental results of Uberoi & Corrsin (1952) (U), Townsend (1954) (T) and Stapountzis *et al.* (1986) (S).

The data collected by Fackrell & Robins (1982) were obtained at travel times in the range $0.26\sigma^2/\epsilon$ to $1.74\sigma^2/\epsilon$, times which the model predicts will lie within the second stage of evolution. The measured σ_c profiles are consistent with this, showing a centreline peak and a similar form to the model profiles. The width of the model's σ_c profile is in good agreement with the experimental data; for the times at which the experimental data was obtained, both the model and the experimental σ_c profile half-widths lie between 1.4 and 1.6 times the half-width of the $\langle c \rangle$ profile.

6.2. *Decaying turbulence*

Figure 10 shows model values of $\sigma_c/\langle c \rangle$ at $x = 0$ for dispersion from an area source in decaying turbulence. As in the stationary case the values are strongly affected by the source size at small times, but become independent of source size at large times. However, in contrast to the results obtained in stationary conditions, $\sigma_c/\langle c \rangle$ approaches a small non-zero constant at large time. If $p_\Delta(\Delta, s\,|\,t)$ is exactly Gaussian for $t \gg s$ then (34) holds and this constant can be expressed as

$$\operatorname*{Lim}_{t/s\to\infty}\left(\frac{(\sigma_1(s\,|\,t))^2}{\sigma_\Delta(s\,|\,t)\,\sigma_\Sigma(s\,|\,t)}-1\right)^{\frac{1}{2}}.$$

As noted at the end of §5, $\sigma_1(s\,|\,t)/\sigma_\Delta(s\,|\,t)$ and $\sigma_1(s\,|\,t)/\sigma_\Sigma(s\,|\,t)$ do not tend to unity as $t\to\infty$. Hence, because $\sigma_1^2 = \frac{1}{2}(\sigma_\Delta^2+\sigma_\Sigma^2)$ and because arithmetic means are greater than geometric ones, this limit is strictly positive. The simulations indicate that the value of this limit is about 0.16.

The results of Warhaft's (1984) experiments on dispersion downstream of a cross-stream line source in decaying grid turbulence are also plotted in figure 10. In the same way as Fackrell & Robins' (1982) continuous compact source was interpreted as an instantaneous line source, the continuous line source of Warhaft's experiment is regarded here as an instantaneous area source. It is not so easy to interpret these experiments as those of Fackrell & Robins (1982) because the Reynolds number is relatively low and the model being considered here cannot account for molecular diffusivity and viscosity explicitly. Molecular diffusion almost certainly results in an effective source size that is much larger than the width of the wire used in the

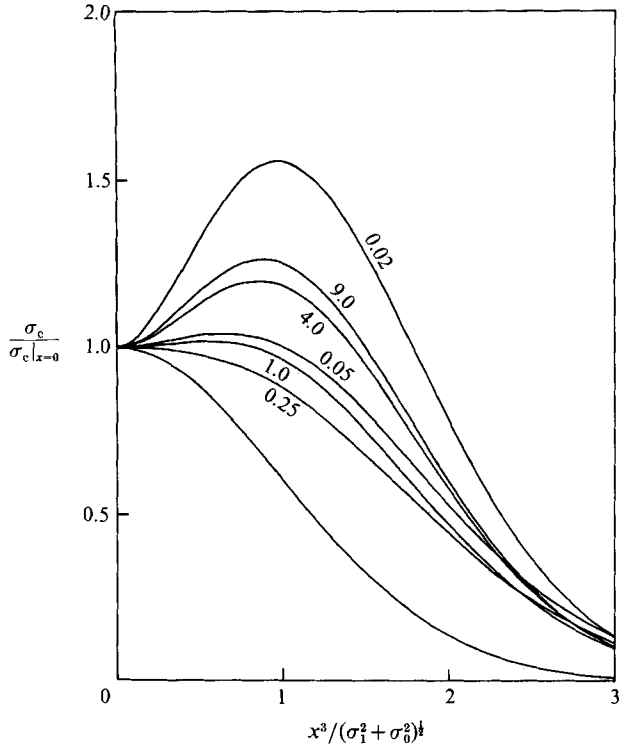

FIGURE 11. Profiles of σ_c from the model for an area source in decaying turbulence. $\sigma_0 = 0.03\sigma_s s$. The numbers attached to the curves indicate values of $(t-s)/s$. The unlabelled curve is a Gaussian distribution with the same standard deviation as the profile of $\langle c \rangle$.

experiments. It seems reasonable to assume that the effective source size will be of the same order as the Kolmogorov microscale, η. The value of η at the source varies between the experiments, lying between $0.01\sigma_s s$ and $0.016\sigma_s s$. The agreement with the model results is best for a slightly larger source size of about $0.03\sigma_s s$. At large times the value of $\sigma_c/\langle c \rangle$ in the model falls off rather too quickly. This is probably because the asymptotic value at large time is too small. Although the agreement could almost certainly be improved by adjusting C_0 and f, it is not proposed to do this here. The agreement is also poor for $(t-s)/s \leqslant 0.02$. This is however to be expected since molecular diffusion must be significant for $(t-s)/s$ of order τ_η/s, a quantity which is about 0.04 in the experiments. To model this region accurately it would be necessary to take account of molecular diffusivity and viscosity explicitly as in Sawford & Hunt (1986) and to use a source size more closely related to the wire diameter. Also shown in figure 10 are the experimental results obtained downwind of a line source in grid turbulence by Uberoi & Corrsin (1952), Townsend (1954) and Stapountzis *et al.* (1986). These data show broadly similar behaviour to Warhaft's data and to the model results.

Figure 11 shows the model profiles of σ_c for $\sigma_0 = 0.03\sigma_s s$. Qualitatively the behaviour is similar to that obtained in stationary conditions (figure 9) and to that observed by Warhaft (1984). At small $(t-s)/s$ the profiles have an off-centre peak, although the model peak is rather more pronounced than in Warhaft's experiments. It seems likely that this discrepancy is due to molecular diffusion which, in the

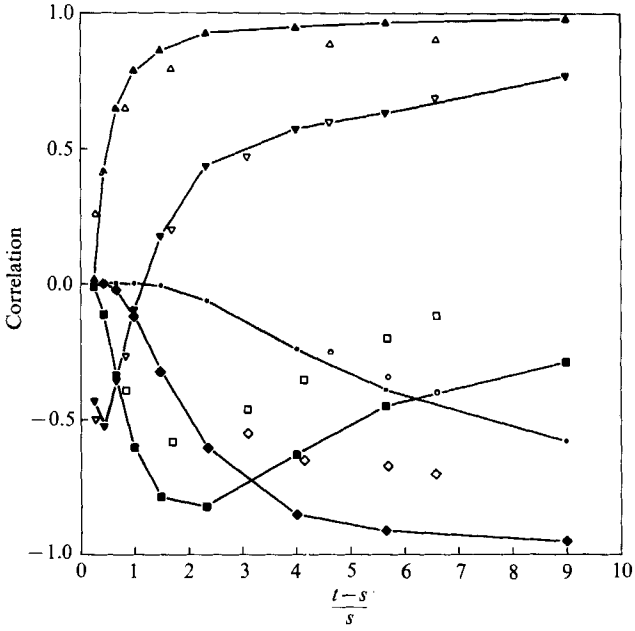

FIGURE 12. Correlation between the concentration resulting from two parallel sources separated by a distance d in decaying turbulence. The correlation is evaluated half way between the two sources. Model results for a source size of $0.03\sigma_s s$ are indicated by solid symbols and experimental results from Warhaft (1984) by open symbols. The different symbol shapes refer to different values of d: ▲, $d = 0.122\sigma_s s$; ▼, $d = 0.4\sigma_s s$; ■, $d = 1.26\sigma_s s$; ◆, $d = 2.52\sigma_s s$; ●, $d = 5.2\sigma_s s$.

experiments, must play a significant role in the early stages of the plume's development. To represent these early stages accurately, it is probably necessary, as above, to use a source size related to the wire diameter and to use a model which includes molecular diffusion and viscous effects explicitly. For $0.11 \leqslant (t-s)/s \leqslant 0.43$ in the model and for $0.073 \leqslant (t-s)/s \leqslant 1.92$ in Warhaft's experiments, the peak is at the centre of the ensemble average plume, with the off-centre peak reappearing at large times. Although the off-centre peak reappears sooner in the model than in the experiments, the model peak value is only a few per cent larger than the centreline value until $(t-s)/s \approx 2$. At large $(t-s)/s$ the model off-centre peak is again rather more pronounced than that measured in the experiments. As noted above, the off-centre peak cannot occur if $\sigma_c/\langle c\rangle$ is as large as unity, and so it seems possible that the more pronounced peak in the model is associated with that fact that the value of $\sigma_c/\langle c\rangle$ in the model is too low at large times. The width of the model σ_c profile is in good agreement with the experimental data, the half width in both the model and the experiments lying between about 1.5 and 2.0 times the half width of the $\langle c\rangle$ profile.

Figures 12 and 13 show model values of the correlation between the concentrations resulting from two parallel instantaneous Gaussian area sources. The sources are taken parallel to the (x^1, x^2)-plane and are separated by a distance d, with the origin (i.e. $\boldsymbol{x} = 0$) lying midway between the sources. Also shown are experimental values for two parallel continuous cross-stream line sources in decaying grid turbulence (Warhaft 1984). As for the single sources considered above, the data is interpreted as relating to two instantaneous area sources. In the model the size of each source was

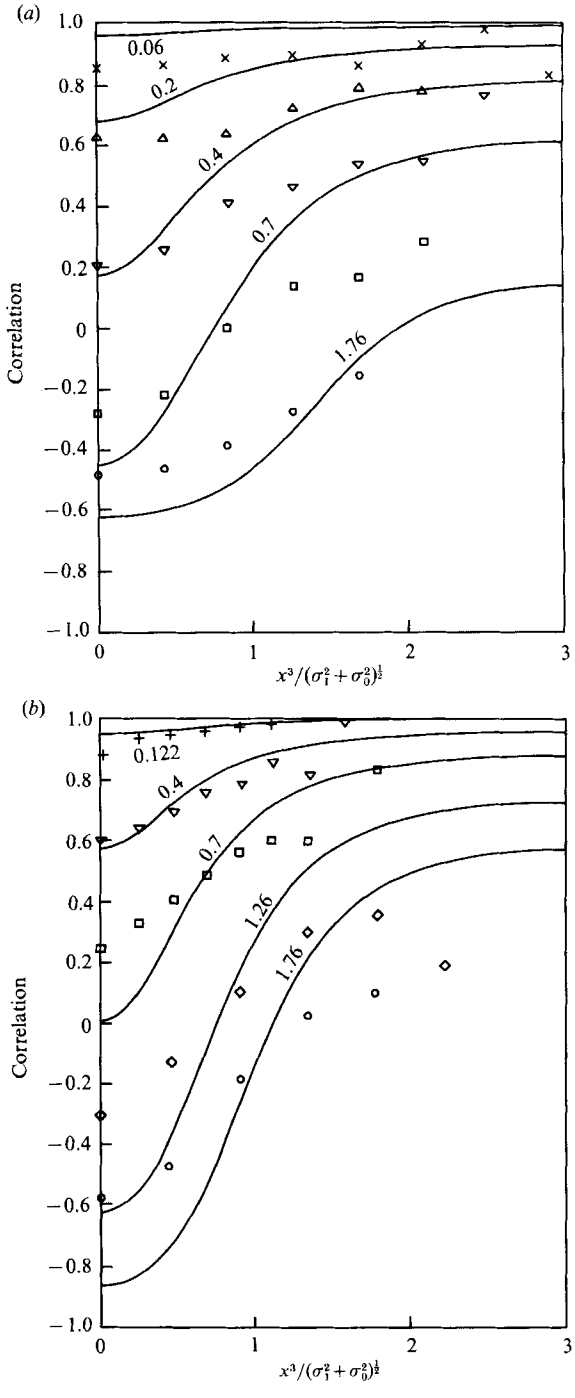

FIGURE 13. Correlation between the concentration resulting from two parallel sources separated by a distance d in decaying turbulence. The correlation is shown as a function of x^3, the origin of x^3 being taken half way between the two sources. (*a*) shows model results for $(t-s)/s = 1.5$ and experimental results (Warhaft 1984) for $(t-s)/s = 1.65$, while (*b*) shows model results for $(t-s)/s = 4.0$ and experimental results for $(t-s)/s = 4.65$. The model results are shown by solid lines and labelled with the value of $d/\sigma_s s$, while the experimental results for different values of d are indicated as follows: $\times$, $d = 0.06\sigma_s s$; $+$, $d = 0.122\sigma_s s$; $\triangle$, $d = 0.2\sigma_s s$; $\triangledown$, $d = 0.4\sigma_s s$; $\square$, $d = 0.7\sigma_s s$; $\diamond$, $d = 1.26\sigma_s s$; $\bigcirc$, $d = 1.76\sigma_s s$. The experimental results are taken from Warhaft's (1984) figure 13 and the values obtained for positive and negative x^3 have been averaged.

taken to be $0.03\sigma_s s$, the value which gives best agreement with the single source data. The values of the correlation at the origin are shown in figure 12. The model values show very similar behaviour to that observed although there are some quantitative differences when the correlation is negative. Figure 13 shows some examples of the correlation at points away from the origin. The agreement between the model and the experiments is again encouraging, although the experimental correlation shows less variation with x^3 than does the correlation from the model.

7. Conclusions

The formulation of two-particle stochastic models has been examined and a new model designed for calculating dispersion in isotropic constant-density flows. The new model yields a well-mixed distribution of particle pairs in $(\boldsymbol{X}, \boldsymbol{U})$-space which is consistent with the constant-density constraint and with a physically reasonable form for the two-point velocity correlation function. Previous models of the form (12) (e.g. Durbin 1980; Lee & Stone 1983) are consistent only with well-mixed distributions which imply $\langle \rho^2 \rangle$ is infinite or which fail to account for the correlation of velocities at neighbouring points. The new model shows a more physically plausible behaviour for the particle separation p.d.f. which, in contrast to previous models of the form (12), agrees with inertial subrange theory. The model is not satisfactory in every respect as it violates the physical constraint (21). However the degree of violation appears to be minor.

Simulations with the new model show that $\sigma_c/\langle c \rangle$ is strongly dependent on source size at small times, but becomes independent of source size at large times. The simulations also suggest that $\sigma_c/\langle c \rangle$ tends to zero in stationary conditions but approaches a small non-zero value in decaying turbulence. However, because of statistical noise, we cannot be certain of the zero limit in the stationary case. The agreement between the model and Fackrell & Robins' (1982) experimental data is encouraging. In particular, varying the source size has the same effect in the model as in the experiments. However the experimental data cannot confirm the zero large-time limit for $\sigma_c/\langle c \rangle$ – indeed it is unlikely that experiments will ever confirm this since, in reality, inhomogeneities or non-stationarities are nearly always important at large times. The agreement with Warhaft's (1984) line source data is not so good, but this may be partly due to the low Reynolds number of the experiments. This data, which was obtained in decaying turbulence, shows clearly a non-zero limit for $\sigma_c/\langle c \rangle$, although the value of this limit is rather larger than the model value. The model also shows encouraging agreement with the data of Warhaft (1984) on the correlation between the concentration from two sources separated in space.

I would like to thank Professor Philip Chatwin for many useful discussions and suggestions. This work forms part of a PhD thesis submitted to Brunel University.

Appendix A. Numerical procedure

The new model described in §4.1 is quite complex to implement because the expression for $\boldsymbol{a}$ contains a large number of terms. In the calculations carried out above, the model was simplified by the method used in the one-particle model of Thomson (1986*a*). This involves using a different set of finite-difference equations at alternate timesteps.

When the particle separation is large, the timescale on which particle velocities change is τ and so we require $\Delta t \ll \tau$ for accurate results. When the particles are close together however, the timescale of the relative motion of particles is much smaller than τ and so a much smaller timestep is required. In order to allow for this and also avoid unnecessary waste of computing resources, the timestep was made a function of the particle separation and was allowed to vary along the particle-pair trajectory. The timestep Δt used in most of the calculations was chosen to be $0.1\tau(1-f(\Delta))$. This ensures that $\Delta t \ll \tau$ at all times and also that $\Delta t \ll (\Delta^2/\epsilon)^{\frac{1}{3}}$ when the particle separation lies in the inertial subrange ($(\Delta^2/\epsilon)^{\frac{1}{3}}$ is the timescale of the eddies which make the dominant contribution to the relative motion of the particles). A few experiments were conducted with a timestep of $0.05\tau(1-f(\Delta))$. This resulted in only small differences (a few per cent) in most statistics. An exception is the statistic $\overline{|\delta\Delta\boldsymbol{x}|^2}$ shown in figure 4. In the case where the initial particle separation was $2\times10^{-3}l$, a timestep of $0.01\tau(1-f(\Delta))$ was found necessary to ensure that the results were independent of Δt. This is to be expected since, with $\Delta t = 0.1\tau(1-f(\Delta))$, the initial timestep is about one third of the time interval between the release of the particles and the time corresponding to the first data point in figure 4. Clearly the quantity $\overline{|\delta\Delta\boldsymbol{x}|^2}$, which depends on the departure of the trajectories from straight lines (and so depends on the difference between two nearly equal quantities), is unlikely to be well represented at the time of the first data point when the timestep is so large.

On the occasions when coincident particles needed to be released an initial separation of $2\times10^{-6}l$ was used. The results appear insensitive to changes in this quantity of an order of magnitude. It is of course impossible to have truly coincident particles since this would necessitate a timestep of length zero.

Thirty thousand particle pairs were followed in all the simulations from which p.d.f.s or concentration statistics were calculated, with the exception of the simulations involving the 'particle splitting' technique for which 10000 pairs were released. The remaining simulations were used only to calculate quantities such as σ_Δ, $\overline{x_1^3}$ or $\overline{|\delta\Delta\boldsymbol{x}|^2}$. For such quantities statistical noise is not a major problem, and so only 10000 pairs were followed in these simulations.

In calculating $\langle c^2\rangle$ with the approximation (31), p_Δ was calculated from simulations which utilized the particle splitting technique, and was represented as a series of straight line segments between data points, each data point representing the average value of p_Δ over a small interval of Δ values. The distance between data points was similar to that used in the graphs shown in figures 1 (*b*) and 5. The use of a much larger distance would tend to smooth the peak in p_Δ observed at small travel times, while a much smaller distance would greatly increase the scatter. For the area and line sources considered in §6, a consequence of (32) and (33) is that σ_c depends on p_Δ only through $\bar{\bar{p}}_\Delta$ and $\bar{p}_\Delta$ respectively. These quantities do not show such a marked peak as p_Δ and so the accuracy of the results might be increased by calculating $\bar{\bar{p}}_\Delta$ and $\bar{p}_\Delta$ with a larger distance between data points as in figures 1 (*d*) and 1 (*e*); however for simplicity this has not been done here.

Appendix B. The relation between $\overline{|\delta \boldsymbol{x}_1|^2}$ and $\overline{|\delta \Delta \boldsymbol{x}|^2}$

In reality, the variance of $\delta \boldsymbol{x}_1$ and $\delta \Delta \boldsymbol{x}$ at time t can be expressed as

$$\overline{|\delta \boldsymbol{x}_1|^2} = \int_s^t \int_s^t \overline{\delta \boldsymbol{u}_1(t_1) \cdot \delta \boldsymbol{u}_1(t_2)}\, \mathrm{d}t_1\, \mathrm{d}t_2,$$

$$\overline{|\delta \Delta \boldsymbol{x}|^2} = \int_s^t \int_s^t \overline{\delta \Delta \boldsymbol{u}(t_1) \cdot \delta \Delta \boldsymbol{u}(t_2)}\, \mathrm{d}t_1\, \mathrm{d}t_2,$$

with

$$\overline{\delta \boldsymbol{u}_1(t_1) \cdot \delta \boldsymbol{u}_1(t_2)} = \int_s^{t_1} \int_s^{t_2} \overline{\boldsymbol{a}_1(s_1) \cdot \boldsymbol{a}_1(s_2)}\, \mathrm{d}s_1\, \mathrm{d}s_2,$$

$$\overline{\delta \Delta \boldsymbol{u}(t_1) \cdot \delta \Delta \boldsymbol{u}(t_2)} = \int_s^{t_1} \int_s^{t_2} \overline{\Delta \boldsymbol{a}(s_1) \cdot \Delta \boldsymbol{a}(s_2)}\, \mathrm{d}s_1\, \mathrm{d}s_2,$$

where $\boldsymbol{a}_i(t)$ is the acceleration of particle i and $\Delta \boldsymbol{a} = (\boldsymbol{a}_1 - \boldsymbol{a}_2)/\sqrt{2}$. As in §5, the average is over particle pairs with a given position in $\boldsymbol{X}$-space at time s. Also $\overline{\Delta \boldsymbol{a}(s_1) \cdot \Delta \boldsymbol{a}(s_2)}$ can be written in the form

$$\overline{\boldsymbol{a}_1(s_1) \cdot \boldsymbol{a}_1(s_2)} - \overline{\boldsymbol{a}_1(s_1) \cdot \boldsymbol{a}_2(s_2)}. \tag{B 1}$$

For simplicity we will only consider the case where the initial separation lies well within the inertial subrange and restrict consideration to travel times over which the evolution of $\delta \boldsymbol{x}_1$ and $\delta \Delta \boldsymbol{x}$ are dominated by inertial subrange eddies (in the model this means, as noted in §5, imposing the restrictions $\Delta(s) \ll l$ and $t - s \ll \tau$). We first recall that the acceleration field is only well-correlated over very short lengthscales of the order of the Kolmogorov microscale η (Monin & Yaglom 1975, §21.5). From this Monin & Yaglom (1975, pp. 546–547) and Sawford (1984) argue that the second term in (B 1) makes a negligible contribution to $\overline{|\delta \Delta \boldsymbol{x}|^2}$ for times $t - s \ll \tau$. If this is so, it follows that $\overline{|\delta \boldsymbol{x}_1|^2} = \overline{|\delta \Delta \boldsymbol{x}|^2}$ for $t - s \ll \tau$. Although it is true that $\overline{\boldsymbol{a}_1(s_1) \cdot \boldsymbol{a}_2(s_2)}$ is small, the following argument suggests that it may not be negligible over such times (note it is clearly not negligible at very large times when $\overline{|\delta \boldsymbol{x}_1|^2} \sim \overline{|\boldsymbol{u}_1(s)|^2}\,(t-s)^2$ and $\overline{|\delta \Delta \boldsymbol{x}|^2} \sim \overline{|\Delta \boldsymbol{u}(s)|^2}\,(t-s)^2$; these cannot be equal unless the initial separation is so large that the initial velocities of the two particles are uncorrelated). In the inertial subrange, the Eulerian acceleration covariance $\langle \boldsymbol{a}(\boldsymbol{x}, t) \cdot \boldsymbol{a}(\boldsymbol{x} + \boldsymbol{r}, t) \rangle$ between the acceleration at two points separated by a distance $r = |\boldsymbol{r}|$ is proportional to $\epsilon^{\frac{4}{3}} r^{-\frac{2}{3}}$ (Monin & Yaglom 1975, p. 371). On dimensional grounds this covariance is expected to persist over a time of order $\epsilon^{-\frac{1}{3}} r^{\frac{2}{3}}$, i.e. we expect $\langle \boldsymbol{a}(\boldsymbol{x}, s_1) \cdot \boldsymbol{a}(\boldsymbol{x} + \boldsymbol{r}, s_2) \rangle$ to be of order $\epsilon^{\frac{4}{3}} r^{-\frac{2}{3}}$ for $|s_1 - s_2| < \epsilon^{-\frac{1}{3}} r^{\frac{2}{3}}$. Provided that the Eulerian and Lagrangian acceleration covariances are of the same order of magnitude and that s_1 lies well inside the interval $[s, t_2]$, this implies that, for two particles with separation r at time s_1,

$$\int_s^{t_2} \overline{\boldsymbol{a}_1(s_1) \cdot \boldsymbol{a}_2(s_2)}\, \mathrm{d}s_2$$

is of order $(\epsilon^{\frac{4}{3}} r^{-\frac{2}{3}})(\epsilon^{-\frac{1}{3}} r^{\frac{2}{3}}) = \epsilon$. It follows that, provided $t - s \gg (\Delta(s)^2/\epsilon)^{\frac{1}{3}}$ (so that the acceleration covariance $\overline{\boldsymbol{a}_1(s_1) \cdot \boldsymbol{a}_2(s_2)}$ has time to act), the contribution to $\overline{|\delta \Delta \boldsymbol{x}|^2}$ from the second term in (B 1) is of order ϵt^3, which is (on dimensional grounds) comparable to $\overline{|\delta \Delta \boldsymbol{x}|^2}$ itself. This suggests that the second term in (B 1) is not negligible and that $\overline{|\delta \Delta \boldsymbol{x}|^2}$ is not equal to $\overline{|\delta \boldsymbol{x}_1|^2}$ for times in the range $(\Delta(s)^2/\epsilon)^{\frac{1}{3}} \ll t - s \ll \tau$.

In fact, for initially coincident particles, $\overline{|\delta \Delta \boldsymbol{x}|^2}$ cannot be greater than $\overline{|\delta \boldsymbol{x}_1|^2}$ and so, if we accept the above argument, must be less than $|\delta \boldsymbol{x}_1|^2$. To see this consider a single realization and consider all particles in the realization which are at $\boldsymbol{y}$ at time s. The

phase space trajectories of such particles will be denoted by $(\boldsymbol{x}(t), \boldsymbol{u}(t))$. The term q_1 will denote the average of $|\boldsymbol{x}(t)-\boldsymbol{y}-\boldsymbol{u}(s)\,(t-s)|^2$ for such particles and q_2 will denote the average of $\frac{1}{2}|\boldsymbol{x}_1(t)-\boldsymbol{x}_2(t)|^2$ for pairs of such particles. q_2 is equal to the mean square of the displacement $|\boldsymbol{x}(t)-\boldsymbol{x}_{\rm CM}(t)|$ of such particles relative to their centre of mass $\boldsymbol{x}_{\rm CM}(t)$ (Batchelor 1952) and so $q_1 = q_2+|\boldsymbol{x}_{\rm CM}(t)-\boldsymbol{y}-\boldsymbol{u}(s)\,(t-s)|^2$ and, in particular, $q_1 \geqslant q_2$. Now, for initially coincident particles, $\delta\Delta\boldsymbol{x} = \Delta\boldsymbol{x}$ and so $\overline{|\delta\boldsymbol{x}_1|^2}$ and $\overline{|\delta\Delta\boldsymbol{x}|^2}$ are equal to the ensemble average of q_1 and q_2 respectively. Hence $\overline{|\delta\boldsymbol{x}_1|^2} \geqslant \overline{|\delta\Delta\boldsymbol{x}|^2}$. Equality is only possible if $\boldsymbol{x}_{\rm CM} = \boldsymbol{y}+\boldsymbol{u}(s)\,(t-s)$ in every realization. This seems unlikely to be true, lending further support to the idea that $\overline{|\delta\Delta\boldsymbol{x}|^2}$ is less than $\overline{|\delta\boldsymbol{x}_1|^2}$.

For pairs of particles which are not initially coincident, it seems likely that the particles will eventually forget their initial separation and behave in the same way as initially coincident particles (Batchelor 1952). On dimensional grounds we expect this to happen after a time of order $(\Delta(s)^2/\epsilon)^{\frac{1}{3}}$ (assuming the initial particle separation is well within the inertial subrange). Hence, in the case of particles which are not initially coincident, the arguments in the previous paragraph support the idea that $\overline{|\delta\Delta\boldsymbol{x}|^2}$ is less than $\overline{|\delta\boldsymbol{x}_1|^2}$ for travel times $t-s$ much greater than $(\Delta(s)^2/\epsilon)^{\frac{1}{3}}$.

REFERENCES

Anand, M. S. & Pope, S. B. 1985 Diffusion behind a line source in grid turbulence. *Turbulent Shear Flows*, vol. 4. Springer.

Batchelor, G. K. 1952 Diffusion in a field of homogeneous turbulence. II. The relative motion of particles. *Proc. Camb. Phil. Soc.* **48**, 345–362.

Batchelor, G. K. 1953 *The Theory of Homogeneous Turbulence*. Cambridge University Press.

Batchelor, G. K. 1959 Small-scale variation of convected quantities like temperature in turbulent fluid. Part 1. General discussion and the case of small conductivity. *J. Fluid Mech.* **5**, 113–133.

Batchelor, G. K., Howells, I. D. & Townsend, A. A. 1959 Small-scale variation of convected quantities like temperature in turbulent fluid. Part 2. The case of large conductivity. *J. Fluid Mech.* **5**, 134–139.

Batchelor, G. K. & Townsend, A. A. 1956 Turbulent diffusion. In *Surveys in Mechanics* (ed. G. K. Batchelor & R. M. Davies), pp. 352–399. Cambridge University Press.

De Baas, A. F., Van Dop, H. & Nieuwstadt, F. T. M. 1986 An application of the Langevin equation for inhomogeneous conditions to dispersion in a convective boundary layer. *Q. J. R. Met. Soc.* **112**, 165–180.

Durbin, P. A. 1980 A stochastic model of two-particle dispersion and concentration fluctuations in homogeneous turbulence. *J. Fluid Mech.* **100**, 279–302.

Durbin, P. A. 1982 Analysis of the decay of temperature fluctuations in isotropic turbulence. *Phys. Fluids* **25**, 1328–1332.

Egbert, G. D. & Baker, M. B. 1984 Comments on paper 'The effect of Gaussian particle-pair distribution functions in the statistical theory of concentration fluctuations in homogeneous turbulence' by B. L. Sawford (Q. J. April 1983, **109**, 339–353). *Q. J. R. Met. Soc.* **110**, 1195–1199.

Fackrell, J. E. & Robins, A. G. 1982 Concentration fluctuations and fluxes in plumes from point sources in a turbulent boundary layer. *J. Fluid Mech.* **117**, 1–26.

Gifford, F. A. 1982 Horizontal diffusion in the atmosphere: A Lagrangian dynamical theory. *Atmos. Environ.* **16**, 505–512.

Hanna, S. R. 1981 Lagrangian and Eulerian time-scale relations in the daytime boundary layer. *J. Appl. Met.* **20**, 242–249.

Haworth, D. C. & Pope, S. B. 1986 A generalised Langevin model for turbulent flows. *Phys. Fluids* **29**, 387–405.

Lamb, R. G. 1981 A scheme for simulating particle pair motions in turbulent fluid. *J. Comp. Phys.* **39**, 329–346.

LEE, J. T. & STONE, G. L. 1983 The use of Eulerian initial conditions in a Lagrangian model of turbulent diffusion. *Atmos. Environ.* **17**, 2477–2481.

LESIEUR, M. 1987 Turbulence in fluids. Dordrecht: Martinus Nijhoff.

LEY, A. J. & THOMSON, D. J. 1983 A random walk model of dispersion in the diabatic surface layer. *Q. J. R. Met. Soc.* **109**, 867–880.

LIN, C. C. & REID, W. H. 1963 Turbulent flow. Theoretical aspects. *Handbuch der Physik*, vol. 8/2. Springer.

MONIN, A. S. & YAGLOM, A. M. 1971 *Statistical Fluid Mechanics*, vol. 1. MIT Press, Cambridge, Mass.

MONIN, A. S. & YAGLOM, A. M. 1975 *Statistical Fluid Mechanics*, vol. 2. MIT Press, Cambridge, Mass.

NEWMAN, G. R., LAUNDER, B. E. & LUMLEY, J. L. 1981 Modelling the behaviour of homogeneous scalar turbulence. *J. Fluid Mech.* **111**, 217–232.

NOVIKOV, E. A. 1963 Random force method in turbulence theory. *Sov. Phys., J. Exp. Theor. Phys.* **17**, 1449–1454.

OBUKHOV, A. M. 1959 Description of turbulence in terms of Lagrangian variables. *Adv. Geophys.* **6**, 113–116.

PASQUILL, F. & SMITH, F. B. 1983 *Atmospheric Diffusion*, 3rd edn. J. Wiley & Sons.

POPE, S. B. 1985 Pdf methods for turbulent reactive flows. *Prog. Energy Combust. Sci.* **11**, 119–192.

POPE, S. B. 1987 Consistency conditions for random walk models of turbulent dispersion. *Phys. Fluids* **30**, 2374–2379.

SAFFMAN, P. G. 1960 On the effect of the molecular diffusivity in turbulent diffusion. *J. Fluid Mech.* **8**, 273–283.

SAWFORD, B. L. 1982 Lagrangian Monte Carlo simulation of the turbulent motion of a pair of particles. *Q. J. R. Met. Soc.* **108**, 207–213.

SAWFORD, B. L. 1983 The effect of Gaussian particle-pair distribution functions in the statistical theory of concentration fluctuations in homogeneous turbulence. *Q. J. R. Met. Soc.* **109**, 339–353.

SAWFORD, B. L. 1984 The basis for, and some limitations of, the Langevin equation in atmospheric relative dispersion modelling. *Atmos. Environ.* **18**, 2405–2411.

SAWFORD, B. L. 1985 Lagrangian statistical simulation of concentration mean and fluctuation fields. *J. Clim. Appl. Met.* **24**, 1152–1166.

SAWFORD, B. L. & HUNT, J. C. R. 1986 Effects of turbulence structure, molecular diffusion and source size on scalar fluctuations in homogeneous turbulence. *J. Fluid Mech.* **165**, 373–400.

SCHUSS, Z. 1980 Theory and applications of stochastic differential equations. J. Wiley & Sons.

STAPOUNTZIS, H., SAWFORD, B. L., HUNT, J. C. R. & BRITTER, R. E. 1986 Structure of the temperature field downwind of a line source in grid turbulence. *J. Fluid Mech.* **165**, 401–424.

SYKES, R. I., LEWELLEN, W. S. & PARKER, S. F. 1984 A turbulent-transport model for concentration fluctuations and fluxes. *J. Fluid Mech.* **139**, 193–218.

TAYLOR, G. I. 1921 Diffusion by continuous movements. *Proc. Lond. Math. Soc.* (2), **20**, 196–211.

THOMSON, D. J. 1986*a* A random walk model of dispersion in turbulent flows and its application to dispersion in a valley. *Q. J. R. Met. Soc.* **112**, 511–530.

THOMSON, D. J. 1986*b* On the relative dispersion of two particles in homogeneous stationary turbulence and the implications for the size of concentration fluctuations at large times. *Q. J. R. Met. Soc.* **112**, 890–894.

THOMSON, D. J. 1987 Criteria for the selection of stochastic models of particle trajectories in turbulent flows. *J. Fluid Mech.* **180**, 529–556.

THOMSON, D. J. 1988 Random walk models of turbulent diffusion. PhD thesis, Brunel University.

TOWNSEND, A. A. 1954 The diffusion behind a line source in homogeneous turbulence. *Proc. R. Soc.* A **224**, 487–512.

TOWNSEND, A. A. 1976 The Structure of Turbulent Shear Flow. Cambridge University Press.

UBEROI, M. S. & CORRSIN, S. 1952 Diffusion of heat from a line source in isotropic turbulence. *National Advisory Committee for Aeronautics, Tech. Note* 2710.

VAN DOP, H., NIEUWSTADT, F. T. M. & HUNT, J. C. R. 1985 Random walk models for particle displacements in inhomogeneous unsteady turbulent flows. *Phys. Fluids* **28**, 1639–1653.

WARHAFT, Z. 1984 The interference of thermal fields from line sources in grid turbulence. *J. Fluid Mech.* **144**, 363–387.

WARHAFT, Z. & LUMLEY, J. L. 1978 An experimental study of the decay of temperature fluctuations in grid-generated turbulence. *J. Fluid Mech.* **88**, 659–684.